NASA Contractor Report 181628

ICASE REPORT NO. 88-8

ICASE

ON THE SMALLEST SCALE FOR THE INCOMPRESSIBLE NAVIER-STOKES EQUATIONS

W. D. Henshaw

H. O. Kreiss

L. G. Reyna

Contract No. NAS1-18107
January 1988

INSTITUTE FOR COMPUTER APPLICATIONS IN SCIENCE AND ENGINEERING
NASA Langley Research Center, Hampton, Virginia 23665

Operated by the Universities Space Research Association

National Aeronautics and
Space Administration

Langley Research Center
Hampton, Virginia 23665

On the smallest scale for the incompressible Navier-Stokes equations

W.D. Henshaw

Mathematical Sciences

IBM Thomas J. Watson Research Center

Yorktown Heights, New York 10598

H.O. Kreiss †

Department of Mathematics

University of California at Los Angeles

Los Angeles, California 90024

L.G. Reyna

Mathematical Sciences

IBM Thomas J. Watson Research Center

Yorktown Heights, New York 10598

Abstract: We prove that for solutions to the two and three dimensional incompressible Navier-Stokes equations the minimum scale is inversely proportional to the square root of the Reynolds number based on the kinematic viscosity and the maximum of the velocity gradients. The bounds on the velocity gradients can be obtained for two dimensional flows, but have to be assumed in three dimensions. Numerical results in two dimensions are given which illustrate and substantiate the features of the proof. Implications of the minimum scale result to the decay rate of the energy spectrum are discussed.

Research was supported in part by the National Aeronautics and Space Administration under NASA Contract No. NAS1-18107 while the second author was in residence at the Institute for Computer Applications in Science and Engineering (ICASE), NASA Langley Research Center, Hampton, VA 23665. Additional support was provided by the National Science Foundation under Grant DMS-8312264 and the Office of Naval Research under Contract N-00014-83-K-0422.

1 Introduction

We consider solutions to the incompressible Navier-Stokes equations

$$\mathbf{u}_t + u\mathbf{u}_x + v\mathbf{u}_y + w\mathbf{u}_z + \nabla p = \nu\Delta\mathbf{u},\ \nu > 0,$$

$$u_x + v_y + w_z = 0,$$

on a 2π-periodic square, where $\mathbf{u} = (u, v, w)$ is the velocity vector, p the pressure and ν the kinematic viscosity. Solutions of the Navier-Stokes equations for small viscosity are usually *turbulent*; such flows posses a lot of structure in both space and time. The viscosity of the fluid controls the level of turbulence within a flow by affecting the energy dissipation. As the viscosity is decreased the size of the smallest features, or scales, diminishes. The relation between the viscosity, the minimum scale and the total energy dissipation is of fundamental interest for the understanding of turbulence.

The mathematical theory for the Navier-Stokes equations is not complete for three dimensional flows: the global regularity is not known and no global bound for the velocity gradients is available. However, both these results are known in two space dimensions. Whether the results from two-dimensional flows are of physical relevance is open to discussion since, in the absence of viscosity, flows in two dimension conserve both energy and enstrophy, while in three dimensions only the energy is conserved. Nevertheless, results on two-dimensional turbulence may be of significance for large scale oceanographic and atmospheric motions.

Assuming global regularity, we relate the minimum scale of the flow to $\overline{|D\mathbf{u}|}_\infty$, the global bound of the velocity gradients. Our main result, precisely stated in theorem (2.1), is that the minimum scale is essentially no smaller than

$$\lambda_{min} = \nu^{1/2}/\overline{|D\mathbf{u}|}_\infty^{\,1/2}.$$

By comparison, a commonly accepted minimum scale for two dimensional flows, λ_{2D}, (see Lilly [19], Orszag [20]), is based on the total dissipation rate of the enstrophy per unit volume. The enstrophy is defined as the square of the L_2-norm of the vorticity. From dimensional arguments it follows that

$$\lambda_{2D} = \nu^{1/2}/\eta^{1/6},$$

where

$$\eta = 2\nu \int\int \|\xi_x\|^2 + \|\xi_y\|^2 dxdy$$

is the total rate of enstrophy dissipation per unit volume and ξ is the vorticity.

In three space dimensions the corresponding minimum scale is the Kolmogoroff dissipation scale [15]

$$\lambda_{3D} = \nu^{3/4}/\epsilon^{1/4},$$

where

$$\epsilon = 2\nu \int\int\int \|\mathbf{u}_x\|^2 + \|\mathbf{u}_y\|^2 + \|\mathbf{u}_z\|^2 dxdydz,$$

is the total rate of energy dissipation per unit volume.

The estimates for the minimum scale can be used to determine the decay rate of the energy spectrum, assuming that a power law does in fact exist.

From our results in two dimensions we conclude that the energy spectrum, $E(k)$, behaves like k^{-3} when there is a maximum rate of enstrophy dissipation in the flow. The k^{-3} power law is in accordance with the Batchelor-Kraichnan theory of enstrophy cascade [3] [16]. The high rate of dissipation can not remain for long times without the flow disappearing. Indeed, numerical experiments show that the solutions rearrange themselves into organized structures which dissipate enstrophy at a much smaller rate. Saffman's work [22], which predicts a power law k^{-4}, seems to describe the behavior of the system at this later stage of evolution. Our theory does not predict the power law but only relates it to the rate of enstrophy dissipation; the k^{-4} law would correspond to η of order $\nu^{1/2}$.

In three space dimensions there is no a priori bound for $\overline{|D\mathbf{u}|}_\infty$. However, if we assume that

$$\overline{|D\mathbf{u}|}_\infty \sim \nu^{-1/2},$$

then when the energy dissipation rate ϵ is of order one, we obtain the Kolmogoroff power law, $E(k) = k^{-5/3}$, and the Kolmogoroff scale $\lambda_{min} = \lambda_{3D} = \nu^{3/4}$.

Some of the first calculations on two-dimensional turbulence were performed by Lilly [19], Fox and Orszag [9], Herring, Orszag, Kraichnan and Fox [12], Fornberg [8], and Barker [1], among others. More recent computations on meshes of up to $1024 \times$

1024 points are described in, for example, Brachet, Sulem [7], Brachet, Meneguzzi, and Sulem [6], Herring, and McWilliams [11] and Benzi *et al* [4]. In some cases the small viscosity limit of the equations was approximated by the continuous removal of the high frequency Fourier coefficients [8]. In other cases the true dissipation term is integrated although some extra smoothing of high frequencies is sometimes required to suppress the growth of aliasing errors [1]. Another approach is to replace the viscosity term by a *super-viscosity*, that is a higher power of the Laplacian operator [7], [11]. This operator allows simulations with a formal viscosity which is much smaller. The minimum scale is nevertheless comparable to the computations presented in this paper.

The numerical simulation of three dimensional flows is still limited by the power of current computing machines. Currently, the largest three dimensional simulations seem to have been performed on 128^3 meshes. However, by exploiting the symmetries of the Taylor-Green problem, Brachet et al. were able to effectively solve with a 256^3 resolution [5]. They find the slope of the spectrum to be least steep when the rate of energy dissipation reaches a maximum. The numerical results seem to agree at this point with the Kolmogoroff scale. For further references on three dimensional computations see the review article by Hussaini and Zang [14].

We restrict ourselves to two dimensional simulations. Our numerical approach has been to attempt to faithfully solve the viscous Navier-Stokes equations. The computations were performed using the pseudo-spectral method, Kreiss and Oliger [18], and Orszag [21]. There is no extra viscosity added to the numerical simulation through smoothing or chopping of the high frequencies, although the fourth-order predictor corrector time integrator produces a small amount of it. Numerical simulations are used to confirm the theoretical estimates and to show that the estimates can be achieved for certain initial conditions. Results are shown for the time development of a flow which initially is maximal dissipative. We also show results of forced problems. In this case there is no easy a priori bound for the maximum norm of the vorticity. We found numerically that the forcing should be proportional to

the viscosity in order to obtain order one velocities. More numerical work on this subject is still necessary.

In section 2 we present the analytical results. In section 3 we present numerical computations in two space dimensions which substantiate and illustrate various features of the proof. Finally, in section 4 we discuss the implications of the minimum scale result to the decay rate of the energy spectrum.

2 Analytical Results

In this section we will prove some results about the rate of decay of the Fourier coefficients for solutions of the incompressible Navier-Stokes equations,

$$\mathbf{u}_t + u\mathbf{u}_x + v\mathbf{u}_y + w\mathbf{u}_z + \nabla p = \nu\Delta\mathbf{u}, \ \nu > 0, \tag{2.1a}$$

$$u_x + v_y + w_z = 0, \tag{2.1b}$$

on the region $\Omega =: \{0 \le x, y, z \le 2\pi\}$ and for $t \ge 0$. We assume that $\mathbf{u} = (u(\mathbf{x}, t), v(\mathbf{x}, t), w(\mathbf{x}, t))$ is 2π-periodic in $\mathbf{x} = (x, y, z)$.

At $t = 0$ we give the initial data

$$\mathbf{u}(\mathbf{x}, 0) = \mathbf{u}_0(\mathbf{x}) \ , \quad \nabla \cdot \mathbf{u}_0 = 0.$$

For simplicity we assume that

$$\int_\Omega \mathbf{u}_0 d\mathbf{x} = 0,$$

which implies

$$\int_\Omega \mathbf{u}(\mathbf{x}, t) d\mathbf{x} = 0 \ , \quad \text{for } t \ge 0. \tag{2.2}$$

We assume that (2.1) has a bounded solution for all times and want to show that the smallest scale is essentially proportional to $(\nu/\overline{|D\mathbf{u}|}_\infty)^{1/2}$. Here

$$\overline{|D\mathbf{u}|}_\infty = \sup_t |D\mathbf{u}|_\infty \quad \text{and} \quad |D\mathbf{u}|_\infty = \sup_{\mathbf{x}} \left(|\partial\mathbf{u}/\partial x|, |\partial\mathbf{u}/\partial y|, |\partial\mathbf{u}/\partial z|\right).$$

In general let

$$D^p\mathbf{u} = \frac{\partial^p \mathbf{u}}{\partial x^{p_1} \partial y^{p_2} \partial z^{p_3}},$$

denote any derivative of $\mathbf{u}$ of order p, where $p = p_1 + p_2 + p_3$.

We are interested in the case when $\nu \ll 1$ and $\overline{|D\mathbf{u}|}_\infty \geq const > 0$. Let us further assume that for every natural number p there is a constant C_p such that the initial conditions satisfy the bounds

$$\max_{0\leq j\leq p} H_j^2(0) =: \max_{0\leq j\leq p} (\|\frac{\partial^j \mathbf{u}}{\partial x^j}(\cdot,0)\|^2 + \|\frac{\partial^j \mathbf{u}}{\partial y^j}(\cdot,0)\|^2) + \|\frac{\partial^j \mathbf{u}}{\partial z^j}(\cdot,0)\|^2) \leq C_p \frac{\overline{|D\mathbf{u}|}_\infty^p}{\nu^p}. \tag{2.3}$$

Here $|\mathbf{f}|_\infty = \sup_{\mathbf{x}\in\Omega} |\mathbf{f}(\mathbf{x})|$ denotes the maximum norm and

$$(\mathbf{f},\mathbf{g}) = \int_\Omega \mathbf{f}\cdot\mathbf{g}\, d\mathbf{x} \quad , \qquad \|\mathbf{f}\|^2 = (\mathbf{f},\mathbf{f}) \, ,$$

the L_2-scalar product and norm. Then we prove

Theorem (2.1): *We assume (2.3) holds and develop* $\mathbf{u}$ *into a Fourier series*

$$\mathbf{u}(\mathbf{x},t) = \sum_{\mathbf{k}} \hat{\mathbf{u}}(\mathbf{k},t) e^{i<\mathbf{k},\mathbf{x}>}, \quad \mathbf{k} = (k_1,k_2,k_3).$$

For every natural number j *and any real number* $\alpha > 0$ *there are constants* K *and* $\tilde{K}$ *which depend on* j, α *and* C_l $(l = l(j,\alpha))$, *such that*

$$\sup_{t\geq 0} |\hat{\mathbf{u}}(k,t)|^2 \leq K \frac{\overline{|D\mathbf{u}|}_\infty^{j+1+\alpha}}{\nu^{j-1+\alpha}\ |k|^{2j}}$$

and

$$\sup_{t\geq 0} |\hat{\mathbf{u}}(k,t)|^2 \leq \tilde{K} \frac{\overline{|D\mathbf{u}|}_\infty^{j+\alpha}}{\nu^{j+\alpha}\ |k|^{2j}}.$$

The estimate of the theorem can be rewritten in the form

$$\sup_{t\geq 0} |\hat{\mathbf{u}}(k,t)|^2 \leq \tilde{K}\ \frac{\overline{|D\mathbf{u}|}_\infty^{\alpha}}{\nu^\alpha} \left\{ \left(\frac{\overline{|D\mathbf{u}|}_\infty}{\nu} \right)^{1/2} \frac{1}{|k|} \right\}^{2j} .$$

We see that the spectrum becomes vanishingly small once $|k| \gg (\overline{|D\mathbf{u}|}_\infty/\nu)^{1/2}$ with $|\hat{\mathbf{u}}(k,t)|$ decaying faster than any power of $(\overline{|D\mathbf{u}|}_\infty/\nu)^{1/2}|k|^{-1}$. It is natural to define the minimum scale of the flow to be proportional to $(\nu/\overline{|D\mathbf{u}|}_\infty)^{1/2}$.

In three space dimensions there is no *a priori* bound for $\overline{|D\mathbf{u}|}_\infty$. One can speculate what the right order of magnitude is. For example, if we assume that

$$\overline{|D\mathbf{u}|}_\infty \sim \nu^{-1/2},$$

we obtain

$$\sup_{t\geq 0} |\hat{\mathbf{u}}(k,t)|^2 \leq \tilde{K}\ \frac{\overline{|D\mathbf{u}|}_\infty^\alpha}{\nu^\alpha}(\nu^{3/4}|k|)^{-2j},$$

which corresponds to the Kolmogoroff scale [19] of $\lambda_{min} = \nu^{3/4}$.

In contrast, for two space dimensions an *a priori* bound for $\overline{|D\mathbf{u}|}_\infty$ can be obtained. The vorticity, $\xi = u_y - v_x$, which satisfies

$$\xi_t + u\xi_x + v\xi_y = \nu\Delta\xi,$$

obeys the maximum principle

$$|\xi|_\infty = \sup_{\mathbf{x},t} |\xi(\mathbf{x},t)| \leq \sup_{\mathbf{x}} |\xi(\mathbf{x},0)|.$$

Therefore, assuming that the initial data satisfy

$$\sup_{\mathbf{x}} |\xi(\mathbf{x},0)| \leq 1, \tag{2.4}$$

we shall prove that $\overline{|D\mathbf{u}|}_\infty$ is essentially bounded independent of ν, in the sense that for every $\beta > 0$ there is a constant $K_1 = K_1(\beta)$ such that

$$|D\mathbf{u}|_\infty \leq K_1\nu^{-\beta}.$$

Thus if the initial data have derivatives of order one then the smallest scale is essentially of the order $\nu^{1/2}$.

Our proof is also valid for Burger's equation. In this case one can prove that

$$|D\mathbf{u}|_\infty \leq const\ \nu^{-1} \sup_{x} |D\mathbf{u}(x,0)|_\infty.$$

Thus our result predicts that the minimum scale is of order ν^{-1}. This bound can be attained in the presence of shocks.

2.1 Estimates for $p \leq 3$

From now on we shall assume that an estimate for $\overline{|D\mathbf{u}|}_\infty$ exists. Integration by parts give us the basic energy estimate

$$\frac{1}{2}\frac{\partial}{\partial t}\|\mathbf{u}\|^2 = -\nu H_1^2,$$

where

$$H_p^2 = H_p^2(t) = \|\frac{\partial^p \mathbf{u}(\cdot,t)}{\partial x^p}\|^2 + \|\frac{\partial^p \mathbf{u}(\cdot,t)}{\partial y^p}\|^2 + \|\frac{\partial^p \mathbf{u}(\cdot,t)}{\partial z^p}\|^2. \tag{2.5}$$

Since by assumption (2.3), $\|\mathbf{u}(\cdot,0)\|^2 \leq const$, it follows

$$2\nu \int_0^\infty H_1^2(t)dt \leq \|\mathbf{u}(\cdot,0)\|^2 \leq const \quad \text{and} \quad \|\mathbf{u}(\cdot,t)\|^2 \leq \|\mathbf{u}(\cdot,0)\|^2 \leq const\ . \tag{2.6}$$

Now differentiate (2.1). For any first space derivative $D\mathbf{u}$ we obtain

$$\frac{1}{2}\frac{\partial}{\partial t}\|D\mathbf{u}\|^2 + I = -\nu(\|D\mathbf{u}_x\|^2 + \|D\mathbf{u}_y\|^2 + \|D\mathbf{u}_z\|^2),$$

where

$$I = (D\mathbf{u}, D(u\mathbf{u}_x + v\mathbf{u}_y + w\mathbf{u}_z)) = II + III,$$

$$II = (D\mathbf{u}, uD\mathbf{u}_x + vD\mathbf{u}_y + wD\mathbf{u}_z),$$

$$III = (D\mathbf{u}, Du\ \mathbf{u}_x + Dv\ \mathbf{u}_y + Dw\ \mathbf{u}_z).$$

Integration by parts and $\nabla \cdot \mathbf{u} = 0$ shows that $II = 0$. Again by integration by parts we obtain

$$III \leq const\ |D\mathbf{u}|_\infty H_1^2.$$

Therefore

$$\frac{1}{2}\frac{\partial}{\partial t}\|D\mathbf{u}\|^2 \leq const\ |D\mathbf{u}|_\infty H_1^2 - \nu(\|D\mathbf{u}_x\|^2 + \|D\mathbf{u}_y\|^2 + \|D\mathbf{u}_z\|^2),$$

that is

$$\frac{1}{2}\frac{\partial}{\partial t}H_1^2 \leq const\ |D\mathbf{u}|_\infty H_1^2 - \nu H_2^2.$$

Integrating the last inequality with respect to t gives us,

$$H_1^2(t) \leq H_1^2(0) + const\ \overline{|D\mathbf{u}|}_\infty \int_0^t H_1^2(\tau)d\tau - 2\nu \int_0^t H_2^2(\tau)d\tau.$$

Therefore by (2.3) and (2.6)

$$H_1^2(t) \leq const\ \frac{\overline{|Du|}_\infty}{\nu} \quad \text{and} \quad \nu \int_0^\infty H_2^2(t)dt \leq const\ \frac{\overline{|Du|}_\infty}{\nu}. \tag{2.7}$$

For the second derivatives we obtain

$$\frac{1}{2}\frac{\partial}{\partial t}\|D^2\mathbf{u}\|^2 + I = -\nu(\|D^2\mathbf{u}_x\|^2 + \|D^2\mathbf{u}_y\|^2 + \|D^2\mathbf{u}_z\|^2),$$

where

$$\begin{aligned}
I &= (D^2\mathbf{u}, D^2(u\mathbf{u}_x + v\mathbf{u}_y + w\mathbf{u}_z)) = II + III + IV,\\
II &= (D^2\mathbf{u}, uD^2\mathbf{u}_x + vD^2\mathbf{u}_y + wD^2\mathbf{u}_z) = 0,\\
III &= 2(D^2\mathbf{u}, DuD\mathbf{u}_x + DvD\mathbf{u}_y + DwD\mathbf{u}_z) \leq const\ |D\mathbf{u}|_\infty H_2^2,\\
IV &= (D^2\mathbf{u}, D^2u\ \mathbf{u}_x + D^2v\ \mathbf{u}_y + D^2w\ \mathbf{u}_z) \leq const\ |D\mathbf{u}|_\infty H_2^2.
\end{aligned}$$

Therefore,

$$\frac{1}{2}\frac{\partial}{\partial t}H_2^2 \leq const\ |D\mathbf{u}|_\infty H_2^2 - \nu H_3^2.$$

Integrating the last inequality with respect to t and using (2.3), (2.7) gives us

$$H_2^2(t) \leq const\ \frac{\overline{|Du|}_\infty^2}{\nu^2} \quad \text{and} \quad \nu \int_0^\infty H_3^2(t)dt \leq const\ \frac{\overline{|Du|}_\infty^2}{\nu^2}. \tag{2.8}$$

For the third derivatives we obtain

$$\frac{1}{2}(D^3\mathbf{u}, D^3\mathbf{u})_t + I = -\nu(\|D^3\mathbf{u}_x\|^2 + \|D^3\mathbf{u}_y\|^2 + \|D^3\mathbf{u}_z\|^2),$$

where by Leibniz's rule

$$\begin{aligned}
I &= (D^3\mathbf{u}, D^3(u\mathbf{u}_x + v\mathbf{u}_y + w\mathbf{u}_z)) = II + III + IV + V,\\
II &= (D^3\mathbf{u}, uD^3\mathbf{u}_x + vD^3\mathbf{u}_y + wD^3\mathbf{u}_z) = 0,\\
III &= 3\ (D^3\mathbf{u}, Du\ D^2\mathbf{u}_x + Dv\ D^2\mathbf{u}_y + Dw\ D^2\mathbf{u}_z) \leq const\ |D\mathbf{u}|_\infty H_3^2,\\
IV &= 3\ (D^3\mathbf{u}, D^2u\ D\mathbf{u}_x + D^2v\ D\mathbf{u}_y + D^2w\ D\mathbf{u}_z) \leq const\ |D\mathbf{u}|_\infty H_4 H_2,\\
V &= (D^3\mathbf{u}, D^3u\ \mathbf{u}_x + D^3v\ \mathbf{u}_y + D^3w\ \mathbf{u}_z) \leq const\ |D\mathbf{u}|_\infty H_3^2.
\end{aligned}$$

Therefore

$$\frac{1}{2}\frac{\partial}{\partial t}H_3^2 \le const\ |D\mathbf{u}|_\infty(H_3^2 + H_4H_2) - \nu H_4^2,$$
$$\le const\ |D\mathbf{u}|_\infty H_3^2 + const\ |D\mathbf{u}|_\infty^2 \frac{H_2^2}{\nu} - \frac{1}{2}\nu H_4^2,$$

thus using (2.3), (2.7) and (2.8)

$$H_3^2(t) \le const\ \frac{\overline{|D\mathbf{u}|}_\infty^3}{\nu^3} \quad \text{and} \quad \nu\int_0^\infty H_4^2(t)dt \le const\ \frac{\overline{|D\mathbf{u}|}_\infty^3}{\nu^3}. \tag{2.9}$$

2.2 The estimates for general p

We now prove theorem (2.1) for arbitrary p. First we obtain energy estimates for H_p in terms of $\overline{|D^j\mathbf{u}|}_\infty$, $1 \le j \le \max(1,[(p-1)/3])$. These estimates are used to obtain bounds for $\overline{|D^j\mathbf{u}|}_\infty$ in terms of $\overline{|D\mathbf{u}|}_\infty$. Finally improved estimates are obtained for H_p, $\overline{|D^p\mathbf{u}|}_\infty$ and $\overline{|D^j\mathbf{u}|}_\infty$ using interpolation inequalities; the theorem then follows. We start with

Lemma (2.1): *For every p there is a constant K_p such that*

$$|(D^p\mathbf{u}, D^p(u\mathbf{u}_x + v\mathbf{u}_y + w\mathbf{u}_z)|$$
$$\le K_p\left(|D\mathbf{u}|_\infty H_p^2 + H_{p+1}\sum_{j=1}^{\max(1,[(p-1)/3])}|D^j\mathbf{u}|_\infty H_{p-j}\right).$$

Here

$$[x] = \textit{largest integer} \le x \quad \text{and} \quad |D^j\mathbf{u}|_\infty = \max_{\mathbf{x},|k|=j}|D^k\mathbf{u}|.$$

Proof: We need to estimate expressions of the form

$$(D^p\mathbf{u}, D^{p-k}u\ D^k\mathbf{u}_x + D^{p-k}v\ D^k\mathbf{u}_y + D^{p-k}w\ D^k\mathbf{u}_z) \quad \text{for} \quad k = 0,\ldots,p-1.$$

We integrate by parts to decrease the order of $D^p\mathbf{u}$. In doing this the order of $D^{p-k}u$, $D^{p-k}v$ and $D^{p-k}w$ or the order of $D^k\mathbf{u}_x$, $D^k\mathbf{u}_y$ and $D^k\mathbf{u}_z$ will increase. For each new term generated through integration by parts,

$$(D^q\mathbf{u}, D^{q_2}u\ D^{q_3}\mathbf{u}_x) + (D^q\mathbf{u}, D^{q_2}v\ D^{q_3}\mathbf{u}_y) + (D^q\mathbf{u}, D^{q_2}w\ D^{q_3}\mathbf{u}_z),$$

we can decrease the order q and increase one of q_2 or q_3 until one of the following conditions is satisfied:

(1) $q-1 \le q_3 \le q$ and $q_2 \le q$

(2) $q \le q_2 \le q+1$ and $q_3 \le q-1$

Note that in case (1) if $q_3 = q$ then

$$(D^q\mathbf{u}, D^{q_2}uD^q\mathbf{u}_x + D^{q_2}vD^q\mathbf{u}_y + D^{q_2}wD^q\mathbf{u}_z) = 0.$$

It follows that

$$I = (D^p\mathbf{u}, D^p(u\mathbf{u}_x + v\mathbf{u}_y + w\mathbf{u}_z)\,)$$

can be written as a sum of terms

$$A := (D^q\mathbf{u}, D^{2p-2q+1}u\ D^{q-1}\mathbf{u}_x + D^{2p-2q+1}v\ D^{q-1}\mathbf{u}_y + D^{2p-2q+1}w\ D^{q-1}\mathbf{u}_z),$$
$$1 \le 2p-2q+1 \le q,$$
$$B := (D^q\mathbf{u}, D^{q+1}u\ D^{2p-2q-1}\mathbf{u}_x + D^{q+1}v\ D^{2p-2q-1}\mathbf{u}_y + D^{q+1}w\ D^{2p-2q-1}\mathbf{u}_z),$$
$$1 \le 2p-2q-1 \le q-1,$$
$$C := (D^q\mathbf{u}, D^qu\ D^{2p-2q}\mathbf{u}_x + D^qv\ D^{2p-2q}\mathbf{u}_y + D^qw\ D^{2p-2q}\mathbf{u}_z),$$
$$0 \le 2p-2q \le q-2.$$

Expression A: If $2p-2q+1=1$ then the estimate follows, otherwise integration by parts is applied to expression A,

$$A = (D^{p-q}u, D^{p-q+1}\,(D^q\mathbf{u}D^{q-1}\mathbf{u}_x)\,) + (D^{p-q}v, D^{p-q+1}\,(D^q\mathbf{u}D^{q-1}\mathbf{u}_y)\,) + (D^{p-q}w, D^{p-q+1}\,(D^q\mathbf{u}D^{q-1}\mathbf{u}_z)\,),$$

to reduce the order of the factors $D^{2p-2q+1}u$, $D^{2p-2q+1}v$ and $D^{2p-2q+1}w$. In this way we can write A as a sum of terms

$$(D^{q_1}\mathbf{u}, D^{p-q}u\ D^{q_2-1}\mathbf{u}_x + D^{p-q}v\ D^{q_2-1}\mathbf{u}_y + D^{p-q}w\ D^{q_2-1}\mathbf{u}_z),$$

where

$$p-q \ge 1, \quad q_j \le p+1, \quad \text{and} \quad q_1+q_2 = p+q+1.$$

Also, $1 \leq 2p - 2q + 1 \leq q$ implies

$$p - q \leq \max\left(1, [\frac{1}{3}(p-1)]\right).$$

The required estimates can be obtained in the following cases:

(i) If $p - q = 1$ then either $q_1 = q_2 = p$ or one of the $q_j = p + 1$ and the other is equal to $p - 1$.

(ii) One of the q_j is equal to $p + 1$.

When neither (i) nor (ii) is satisfied then $q_j < p + 1$ and $p - q > 1$, and we can reduce D^{p-q} further. This shows that A can be estimated in the desired way.

Expression B: Correspondingly, by reducing the order of $D^{2p-2q-1}\mathbf{u}_x$, $D^{2p-2q-1}\mathbf{u}_y$ and $D^{2p-2q-1}\mathbf{u}_z$, B can be written as sum of terms

$$(D^{q_1}\mathbf{u}, D^{q_2}u\ D^{p-q-1}\mathbf{u}_x + D^{q_2}v\ D^{p-q-1}\mathbf{u}_y + D^{q_2}w\ D^{p-q-1}\mathbf{u}_z) := II,$$

where

$$q_j \leq p+1\ , \quad q_1 + q_2 = p + q + 1 \quad \text{and} \quad p - q - 1 \geq 0.$$

Also $2p - 2q \leq q$ implies $0 \leq p - q - 1 \leq [\frac{1}{3}(p-3)]$. II can be estimated in the following two cases:

(i) If $p - q - 1 = 0$ then $q_1 = p + 1$, $q_2 = p - 1$ or $q_1 = q_2 = p$, and

$$II \leq const\ |D\mathbf{u}|_\infty H_{p+1} H_{p-1}, \quad \text{or}$$

$$II \leq const\ |D\mathbf{u}|_\infty H_p^2.$$

(ii) If $q_1 = p + 1$ or $q_2 = p + 1$.

Otherwise $q_j < p+1$ and $p-q-1 > 0$ and hence we can diminish $p-q-1$ further. Therefore we obtain the desired estimates for B.

Expression C: Integration by parts allows us to diminish the order of $D^{2p-2q}\mathbf{u}$ obtaining terms of the form

$$(D^{q_1}\mathbf{u}, D^{q_2}u\ D^{p-q-1}\mathbf{u}_x + D^{q_2}v\ D^{p-q-1}\mathbf{u}_y + D^{q_2}w\ D^{p-q-1}\mathbf{u}_z)$$

where

$$q_j < p+1\ , \quad q_1 + q_2 = p + q + 1 \quad \text{and} \quad p - q - 1 \geq 0.$$

Using the same argument as for B we obtain the desired estimate. This proves the lemma.

Differentiating (2.1) p-times gives us

$$\frac{1}{2}\frac{\partial}{\partial t}(D^p\mathbf{u}, D^p\mathbf{u}) + (D^p\mathbf{u}, D^p(u\mathbf{u}_x + v\mathbf{u}_y + w\mathbf{u}_z)\,) \\ = -\nu(\|D^p\mathbf{u}_x\|^2 + \|D^p\mathbf{u}_y\|^2 + \|D^p\mathbf{u}_z\|^2)$$

Therefore we obtain from lemma (2.1)

$$\frac{\partial}{\partial t}H_p^2 \leq const\ \left(|D\mathbf{u}|_\infty H_p^2 + H_{p+1}\sum_{j=1}^{\max(1,[(p-1)/3])}|D^j\mathbf{u}|_\infty H_{p-j}\right) - 2\nu H_{p+1}^2$$

$$\leq const\ \left(|D\mathbf{u}|_\infty H_p^2 + \frac{1}{\nu}\sum_{j=1}^{\max(1,[(p-1)/3])}|D^j\mathbf{u}|_\infty^2 H_{p-j}^2\right) - \nu H_{p+1}^2$$

Using the notation

$$L_p = \int_0^\infty H_p^2(t)dt$$

the last inequality implies

$$H_p^2(t) \leq const\ \left(\frac{\overline{|D\mathbf{u}|}_\infty^p}{\nu^p} + \overline{|D\mathbf{u}|}_\infty L_p + \frac{1}{\nu}\sum_{j=1}^{\max(1,[(p-1)/3])}\overline{|D^j\mathbf{u}|}_\infty^2 L_{p-j}\right) \qquad (2.10)$$

and

$$L_{p+1} \leq const\ \left(\frac{\overline{|D\mathbf{u}|}_\infty^p}{\nu^{p+1}} + \frac{\overline{|D\mathbf{u}|}_\infty}{\nu}L_p + \frac{1}{\nu^2}\sum_{j=1}^{\max(1,[(p-1)/3])}\overline{|D^j\mathbf{u}|}_\infty^2 L_{p-j}\right) \qquad (2.11)$$

To begin with let us obtain estimates for H_p and L_{p+1}, for $p = 4, \ldots, 7$. In most applications this is all what is needed. From our previous results we know that

$$L_3 \leq const\ \frac{\overline{|D\mathbf{u}|}_\infty^2}{\nu^3} \quad \text{and} \quad L_4 \leq const\ \frac{\overline{|D\mathbf{u}|}_\infty^3}{\nu^4}.$$

Therefore (2.10) and (2.11) give us

$$H_4^2(t) \leq const\ \left(\frac{\overline{|D\mathbf{u}|}_\infty^4}{\nu^4} + \overline{|D\mathbf{u}|}_\infty L_4 + \frac{1}{\nu}\overline{|D\mathbf{u}|}_\infty^2 L_3\right) \leq const\ \frac{\overline{|D\mathbf{u}|}_\infty^4}{\nu^4},$$

$$L_5 \leq const\ \left(\frac{\overline{|D\mathbf{u}|}_\infty^4}{\nu^5} + \frac{\overline{|D\mathbf{u}|}_\infty}{\nu}L_4 + \frac{1}{\nu^2}\overline{|D\mathbf{u}|}_\infty^2 L_3\right) \leq const\ \frac{\overline{|D\mathbf{u}|}_\infty^4}{\nu^5},$$

The estimates for H_5^2, L_6, H_6^2 and L_7 follow in the same way.

For $p = 7$ we obtain

$$H_7^2(t) \leq const \left(\frac{\overline{|Du|}_\infty^7}{\nu^7} + \overline{|Du|}_\infty L_7 + \frac{1}{\nu}\overline{|Du|}_\infty^2 L_6 + \frac{1}{\nu}\overline{|D^2\mathbf{u}|}_\infty^2 L_5 \right).$$

Thus we have to estimate $|D^2\mathbf{u}|_\infty^2$. By Sobolev inequalities

$$|D^p\mathbf{u}|_\infty^2 \leq \epsilon H_{p+3}^2 + \frac{const}{\epsilon} H_p^2$$

and we obtain for $\epsilon = H_p/H_{p+3}$

$$|D^p\mathbf{u}|_\infty^2 \leq const\ H_{p+3}H_p. \tag{2.12}$$

In particular

$$|D^3\mathbf{u}|_\infty^2 \leq const\ H_6H_3 \leq const\ \frac{\overline{|Du|}_\infty^{9/2}}{\nu^{9/2}}$$

Now we use the usual interpolation inequality (see for example [10])

$$|D^j\mathbf{u}|_\infty^2 \leq \epsilon|D^p\mathbf{u}|_\infty^2 + const\ \epsilon^{-(j-1)/(p-j)}|Du|_\infty^2, \quad 1 \leq j < p$$

which gives us for $\epsilon = (|Du|_\infty^2/|D^p\mathbf{u}|_\infty^2)^{(p-j)/(p-1)}$

$$|D^j\mathbf{u}|_\infty^2 \leq const\ (|D^p\mathbf{u}|_\infty^2)^{(j-1)/(p-1)}(|Du|_\infty^2)^{(p-j)/(p-1)}. \tag{2.13}$$

For $j = 2$, $p = 3$ we obtain

$$|D^2\mathbf{u}|_\infty^2 \leq const\ (|D^3\mathbf{u}|_\infty^2)^{1/2}(|Du|_\infty^2)^{1/2} \leq const\ \frac{\overline{|Du|}_\infty^{13/4}}{\nu^{9/4}} \tag{2.14}$$

Therefore

$$H_7^2(t) \leq const\ \frac{\overline{|Du|}_\infty^{7+1/4}}{\nu^{8+1/4}} \quad \text{and} \quad L_8 \leq const\ \frac{\overline{|Du|}_\infty^{7+1/4}}{\nu^{9+1/4}}.$$

Using (2.14) we can in the same way estimate H_8^2 and H_9^2. These estimates are not as sharp as required by theorem (2.1). To obtain the required estimates we have to estimate H_p^2 for general p and then improve the lower order estimates using interpolation inequalities.

Using (2.10) and (2.11) recursively and the estimates for H_p and L_{p+1} for $p \le 6$ we obtain

Lemma (2.2):

$$H_{p+1}^2 \le const \sum_{j_1 \dots j_k} \frac{\overline{|D^{j_1}\mathbf{u}|}_\infty^2 \dots \overline{|D^{j_k}\mathbf{u}|}_\infty^2 \overline{|D\mathbf{u}|}_\infty^{\tau_k - 2k}}{\nu^{\tau_k}}, \tag{2.15}$$

where the sum is over all $\{k, j_i, p_i, q_i\}$ *satisfying the constraints*

$$\tau_k = p + 1 - \sum_{i=1}^{k}(j_i - 1) = 2k + \sum_{i=0}^{k} q_i,$$

$$1 \le j_i \le [p_i/3] \quad , \quad p_{i+1} = p_i - j_i - 1 - q_i \quad , \quad 0 \le q_i \le p_i - j_i \quad \text{for} \quad i = 1, \dots, k$$

$$0 \le q_0 \le p + 1 \quad , \quad q_k = p_k - j_k \quad , \quad p_1 = p - q_0 \quad , \quad k \ge 0.$$

Note that $\tau_k = p + 1$ *for* $p \le 5$.

Proof: We first obtain estiamtes for L_{p+2} from (2.11). H_{p+1}^2 is bounded by ν times this estimate for L_{p+2}.

$$L_{p+2} \le const \left(\overline{|D\mathbf{u}|}_\infty^{p+1}/\nu^{p+2} + (\overline{|D\mathbf{u}|}_\infty/\nu) L_{p+1} + \nu^{-2} \sum_{j=1}^{\max(1,[p/3])} \overline{|D^j\mathbf{u}|}_\infty^2 L_{p+1-j} \right)$$

$$\le const \underbrace{\left(\quad A \quad + \quad B \quad + \quad \right.}_{C} \left. \right),$$

where we have labeled the three terms on the right hand side as A, B and C. In the recursive reduction of L_{p+2} we must consider all possible terms which may arise; at each new stage one must consider the effect of using expression A, B or C. In the general case one chooses B q_0-times followed by term C with $j = j_1$, then B q_1-times, C with $j = j_2$ and so on until finally finishing with term A or B and using the estimates for L_p with $p \le 6$. In this fashion the general term will be

$$\frac{\overline{|D\mathbf{u}|}_\infty^{q_0}}{\nu^{q_0}} \frac{\overline{|D^{j_1}\mathbf{u}|}_\infty^2}{\nu^2} \frac{\overline{|D\mathbf{u}|}_\infty^{q_1}}{\nu^{q_1}} \frac{\overline{|D^{j_2}\mathbf{u}|}_\infty^2}{\nu^2} \cdots \frac{\overline{|D\mathbf{u}|}_\infty^{q_k}}{\nu^{q_k+1}}$$

$$= \overline{|D^{j_1}\mathbf{u}|}_\infty^2 \dots \overline{|D^{j_k}\mathbf{u}|}_\infty^2 \frac{\overline{|D\mathbf{u}|}_\infty^{\Sigma q_i}}{\nu^{\Sigma q_i + 2k + 1}}$$

We define $\tau_k = 2k + \sum q_i$. The constraints on j_i, q_i and p_i follow from the manner in which the general term was obtained.

Now we use (2.13) to estimate $\overline{|D^{j_i}\mathbf{u}|}_\infty^2$ in terms of $\overline{|D^{p-1}\mathbf{u}|}_\infty$ and $\overline{|D\mathbf{u}|}_\infty$,

$$H_{p+1}^2(t) \le const \sum_{j_1 \cdots j_k} \overline{|D^{p-1}\mathbf{u}|}_\infty^{2\sum \frac{j_i-1}{p-2}} \overline{|D\mathbf{u}|}_\infty^{2\sum \frac{p-1-j_i}{p-2}} \frac{\overline{|D\mathbf{u}|}_\infty^{\tau_k-2k}}{\nu^{\tau_k}},$$

$$\le const \sum_{j_1 \cdots j_k} \overline{|D^{p-1}\mathbf{u}|}_\infty^{2(1-\frac{\tau_k-3}{p-2})} \frac{\overline{|D\mathbf{u}|}_\infty^{1+p(\tau_k-3)/(p-2)}}{\nu^{\tau_k}}.$$

Therefore by (2.2) and Sobolev inequalities

$$\overline{|D^{p-1}\mathbf{u}|}_\infty^2 \le const\ (H_{p+1}^2 + H_{p-1}^2)$$

$$\le const\ H_{p+1}^2$$

$$\le const\ \max_{\tau_k} \left(\overline{|D^{p-1}\mathbf{u}|}_\infty^{2(1-\frac{\tau_k-3}{p-2})} \frac{\overline{|D\mathbf{u}|}_\infty^{1+p(\tau_k-3)/(p-2)}}{\nu^{\tau_k}} \right).$$

It follows that

$$\overline{|D^{p-1}\mathbf{u}|}_\infty^2 \le const\ \max_{\tau_k} \left(\frac{\overline{|D\mathbf{u}|}_\infty^{p+\frac{p-2}{\tau_k-3}}}{\nu^{(p-2)\frac{\tau_k}{\tau_k-3}}} \right).$$

One more application of the interpolation inequalities gives for $1 \le j \le p-1$

$$\overline{|D^j\mathbf{u}|}_\infty^2 \le const\ \max_{\tau_k} \left(\frac{\overline{|D\mathbf{u}|}_\infty^{j+1+\frac{j-1}{\tau_k-3}}}{\nu^{\,j-1+3\frac{j-1}{\tau_k-3}}} \right).$$

In order to obtain our final estimate we need to show that that $\overline{\tau} = \min_k \tau_k$ tends to infinity as p tends to infinity. Recall that

$$\tau_k = p + 1 - \sum_{i=1}^{k}(j_i - 1) = 2k + \sum_{i=0}^{k} q_i,$$

$$1 \le j_i \le [p_i/3] \ , \quad p_{i+1} = p_i - j_i - 1 - q_i \ , \quad 0 \le q_i \le p_i - j_i \ \text{ for } \ i = 1, \ldots, k$$

$$0 \le q_0 \le p+1 \ , \quad q_k = p_k - j_k \ , \quad p_1 = p - q_0 \ , \quad k \ge 0.$$

From $j_i \le [p_i/3] \le p_i/3$ it follows that

$$p_{i+1} \ge p_i - \frac{2}{3}p_i - 1 - q_i,$$

$$\Rightarrow (p_{i+1} + 3) \ge \frac{2}{3}(p_i + 3) - q_i,$$

$$\Rightarrow (p_k + 3) \ge (\frac{2}{3})^{k-1}(p+3) - \sum_{i=0}^{k-1}(\frac{2}{3})^{k-1-i} q_i$$

This last expression can be written as

$$k \geq 1 + \log_{3/2}\left(\frac{(p+3) - \sum_{i=0}^{k-1}(\frac{3}{2})^i q_i}{p_k + 3}\right).$$

Since $q_k = p_k - j_k \geq (2/3)p_k$ we have

$$\tau_k = 2k + \sum_{i=0}^{k} q_i \geq 2k + \frac{2}{3}p_k + \sum_{i=0}^{k-1} q_i.$$

Now consider the two cases

(i) $\sum_{i=0}^{k-1}(3/2)^i q_i > (p+3)/2$

(ii) $\sum_{i=0}^{k-1}(3/2)^i q_i \leq (p+3)/2$

In case (i) it follows that

$$\sum_{i=0}^{k-1}(3/2)^{k-1} q_i \geq \sum_{i=0}^{k-1}(3/2)^i q_i > (p+3)/2$$

$$\Rightarrow \sum_{i=0}^{k-1} q_i > (2/3)^{k-1}(p+3)/2$$

$$\Rightarrow \tau_k \geq 2k + (2/3)^{k-1}(p+3)/2$$

Minimizing this last expression with respect to k (≥ 0) gives

$$\tau_k \geq const \ \log(p) \quad \text{for some } const \ > 0.$$

In case (ii) we have

$$k \geq 1 + \log_{3/2}(\frac{p+3}{2(p_k+3)})$$

$$\Rightarrow \tau_k \geq 2 + 2\log_{3/2}(\frac{p+3}{2(p_k+3)}) + (2/3)p_k$$

Since $0 \leq p_k \leq p+1$ it follows that as a function of p_k, the above expression has the bound

$$\tau_k \geq const \ \log(p) \quad \text{for some } const \ > 0.$$

Hence $\bar{\tau} = \min_k \tau_k \geq \delta \log(p)$ as p tends to infinity, for some constant $\delta > 0$. Thus

Theorem (2.2): *For every $j \geq 1$ and any $\alpha > 0$, we can choose p sufficiently large so that*

$$\overline{|D^j \mathbf{u}|}_\infty^2 \leq const \ \frac{\overline{|D\mathbf{u}|}_\infty^{j+1+\alpha}}{\nu^{\,j-1+\alpha}}, \tag{2.16}$$

where the constant depends on p and C_{p+1} introduced in the estimates for the initial conditions (2.3) .

By using (2.16) in (2.15) we obtain

Theorem (2.3): *For every $j \geq 1$ and any $\alpha > 0$, we can choose p sufficiently large so that*

$$H_j^2(t) \leq const \ \frac{\overline{|D\mathbf{u}|}_\infty^{j+\alpha}}{\nu^{\,j+\alpha}}, \tag{2.17}$$

where the constant depends on p and C_{p+1} .

Using the simple estimates for H_j^2 in terms of maximum norms gives

Theorem (2.4): *For every $j \geq 1$ and any $\alpha > 0$, we can choose p sufficiently large so that*

$$H_j^2(t) \leq const \ \frac{\overline{|D\mathbf{u}|}_\infty^{j+1+\alpha}}{\nu^{\,j-1+\alpha}}. \tag{2.18}$$

where the constant depends on p and C_{p+1} .

Theorem (2.1) now follows from Parseval's relation.

It may seem curious that the initial conditions satisfy

$$H_j^2(0) \leq const \ \frac{\overline{|D\mathbf{u}|}_\infty^{j}}{\nu^{\,j}},$$

while we are able to prove that (2.18) holds. However, (2.18) can be derived from (2.17) as follows (for convenience we drop the α's) :

$$H_j^2 \leq const \ \frac{\overline{|D\mathbf{u}|}_\infty^{j}}{\nu^{\,j}}$$

$$\Rightarrow |D^p \mathbf{u}|_\infty^2 \leq const \ H_{p+2}^2 \leq const \ \frac{\overline{|D\mathbf{u}|}_\infty^{p+2}}{\nu^{\,p+2}}$$

and thus using the interpolation inequality (2.13)

$$\begin{aligned} |D^j \mathbf{u}|_\infty^2 &\leq const \ (|D^p \mathbf{u}|_\infty^2)^{(j-1)/(p-1)} (|D\mathbf{u}|_\infty^2)^{(p-j)/(p-1)} \\ &\leq const \ (\frac{|D\mathbf{u}|_\infty^{p+2}}{\nu^{p+2}})^{(j-1)/(p-1)} (|D\mathbf{u}|_\infty^2)^{(p-j)/(p-1)} \\ &\leq const \ \frac{\overline{|D\mathbf{u}|}_\infty^{j+1+\alpha}}{\nu^{\,j-1+\alpha}} \end{aligned}.$$

(2.18) now follows.

2.3 Estimates for two space dimensions

In this section we obtain a sharp bound for $\overline{|D\mathbf{u}|}_\infty$ for two dimensional flows. In this case the incompressible Navier-Stokes equations can be written in vorticity form

$$\xi_t + u\xi_x + v\xi_y = \nu\Delta\xi \quad , \quad \nu > 0, \tag{2.19a}$$

$$u_x + v_y = 0 \quad , \quad u_y - v_x = \xi, \tag{2.19b}$$

where ξ is the vorticity and u, v are the velocity components.

Lemma (2.2): *The solutions of (2.19) satisfy the maximum principle*

$$|\xi(\cdot,t)|_\infty \leq |\xi(\cdot,0)|_\infty.$$

Proof: This well known result follows from the fact that at a local maximum (minimum) of ξ, $\xi_x = \xi_y = 0$ and $\xi_t \leq 0$ (≥ 0).

We would first like to show that $|D\mathbf{u}|_\infty$ is bounded for all time. Note that our energy estimates of the previous section are still valid if we integrate to $t = T > 0$ instead of integrating to $t = \infty$. For this section only, let us redefine the quantities which depend on this bound on the time. For example we define

$$\overline{|D\mathbf{u}|}_\infty = \sup_{t\leq T} |D\mathbf{u}|_\infty \quad \text{and} \quad L_p = \int_0^T H_p^2(t)dt.$$

We know from basic results that $|D\mathbf{u}|_\infty$ exists and is bounded for some finite time interval $[0,T]$. We will now derive estimates for $\overline{|D\mathbf{u}|}_\infty$ which are independent of T. It follows from the results of the previous section that we can obtain estimates for all derivatives which are also independent of T. Then from well known results we can conclude that $|D\mathbf{u}|_\infty$ exists and satisfies these same bounds for all times.

Lemma (2.3): *For any $\alpha_1 > 0$ there exists a constant $C(\alpha_1)$ such that*

$$\overline{|D\mathbf{u}|}_\infty = \sup_{t\leq T} |D\mathbf{u}|_\infty \leq C(\alpha_1)|\xi(\cdot,0)|_\infty^{1+\alpha_1}\nu^{-\alpha_1}. \tag{2.20}$$

Proof: For any β with $0 < \beta < 1$ we define the Hölder semi-norm by

$$|D^\beta f|_\infty = \sup_{\mathbf{x}_1, \mathbf{x}_2 \in \Omega} \frac{|f(\mathbf{x}_1) - f(\mathbf{x}_2)|}{|\mathbf{x}_1 - \mathbf{x}_2|^\beta}.$$

Using the notation

$$|D^\beta \mathbf{u}|_\infty = \max\{|D^\beta u|_\infty, |D^\beta v|_\infty\}$$

the usual Hölder estimates for the solutions of Laplace's equation (see for example [10]), tell us that for any $\beta > 0$ there is a constant $\tilde{C}(\beta)$ such that

$$|D^{1-\beta}\mathbf{u}|_\infty \leq \tilde{C}(\beta)|\xi|_\infty. \tag{2.21}$$

Also, the convexity of Hölder norms (see [13])

$$|D^{k+\alpha} f|_\infty \leq const\ |D^{k_1+\alpha_1} f|_\infty^t |D^{k_2+\alpha_2} f|_\infty^{1-t},$$

$$k + \alpha = t(k_1 + \alpha_1) + (1-t)(k_2 + \alpha_2) \geq 1, \quad 0 < t < 1, \quad \alpha, \alpha_1, \alpha_2 \geq 0,$$

and Young's inequality give us for any $\epsilon > 0$

$$|D\mathbf{u}|_\infty \leq \epsilon |D^2\mathbf{u}|_\infty + const\ \ \epsilon^{-\beta} |D^{1-\beta}\mathbf{u}|_\infty.$$

Using the Sobolev inequality (2.12) for $\overline{|D^2\mathbf{u}|}_\infty$ and (2.21) we obtain

$$\begin{aligned}
\overline{|D\mathbf{u}|}_\infty &\leq const\ \epsilon \frac{\overline{|D\mathbf{u}|}_\infty^{7/2}}{\nu^{7/2}} + const\ \ \epsilon^{-\beta} \overline{|D^{1-\beta}\mathbf{u}|}_\infty, \\
&\leq const\ \left(\epsilon \frac{\overline{|D\mathbf{u}|}_\infty^{7/2}}{\nu^{7/2}} + \epsilon^{-\beta} \tilde{C}(\beta) \overline{|\xi|}_\infty \right).
\end{aligned}$$

Choosing

$$\epsilon^{1+\beta} = \tilde{C}(\beta)\overline{|\xi|}_\infty \frac{\nu^{7/2}}{\overline{|D\mathbf{u}|}_\infty^{7/2}},$$

gives

$$\overline{|D\mathbf{u}|}_\infty \leq const\ \tilde{C}(\beta)\overline{|\xi|}_\infty \left(\tilde{C}(\beta)\overline{|\xi|}_\infty \frac{\nu^{7/2}}{\overline{|D\mathbf{u}|}_\infty^{7/2}} \right)^{-\frac{\beta}{1+\beta}}$$

Thus

$$\overline{|D\mathbf{u}|}_\infty \leq const \left(\tilde{C}(\beta)\overline{|\xi|}_\infty\right)^{1/(1-5\beta/2)} \nu^{-7\beta/(2-5\beta)}$$

and the lemma follows since $\overline{|\xi|}_\infty \leq |\xi(\cdot,0)|_\infty$.

In two space dimensions estimates on the vorticity appear more naturally. In [17] we proved the results of theorem (2.1) in the two-dimensional case using the vorticity formulation of the equations. In that paper the quantities

$$J_p^2(t) = \|\frac{\partial^p \xi}{\partial x^p}\|^2 + \|\frac{\partial^p \xi}{\partial y^p}\|^2 \tag{2.22}$$

take the place of the H_p^2. The estimate corresponding to (2.18) is

$$J_p^2(t) \leq const\ H_{p+1}^2(t) \leq const\ \frac{\overline{|D\mathbf{u}|}_\infty^{p+2+\alpha}}{\nu^{p+\alpha}}. \tag{2.23}$$

We refer to the J_p in the section on numerical results.

3 Numerical Results

We first describe the procedure we use to numerically solve the two-dimensional Navier-Stokes equations. In brief, we discretize in space using the Fourier (pseudo-spectral) method and solve in time using a fourth order predictor-corrector method. The equations are solved in Fourier space and the diffusion term $\nu\Delta\omega$ is treated in a fully implicit manner. We now proceed to present more details.

We solve the two-dimensional incompressible Navier-Stokes equations in the vorticity stream function formulation:

$$\xi_t + (u\xi)_x + (v\xi)_y = \nu\Delta\xi + f \tag{3.1a}$$

$$\Delta\psi = -\xi, \qquad (u,v) = (\psi_y, -\psi_x). \tag{3.1b}$$

The computational domain is taken to be a 2π periodic square. The solution is represented as a truncated Fourier series with ω denoting the discrete approximation to ξ and $\hat{\omega}$ denoting the discrete Fourier transform of ω:

$$\omega(x,y,t) = \sum_{-\frac{1}{2}N_1+1}^{\frac{1}{2}N_1-1} \sum_{-\frac{1}{2}N_2+1}^{\frac{1}{2}N_2-1} \hat{\omega}(k_1,k_2,t)e^{i(k_1x+k_2y)}.$$

Similarly the Fourier transform of ψ and f are denoted by $\hat{\psi}$ and $\hat{f}$ respectively. The equation for the Fourier coefficient $\hat{\omega}(k_1,k_2,t)$ is

$$\hat{\omega}_t + ik_1\widehat{(u\omega)} + ik_2\widehat{(v\omega)} = -\nu(k_1^2+k_2^2)\hat{\omega} + \hat{f} \tag{3.2a}$$

$$(k_1^2+k_2^2)\hat{\psi} = \hat{\omega} \tag{3.2b}$$

The convolutions $\widehat{u\omega}$ and $\widehat{v\omega}$ (i.e. the Fourier transforms of the products $u\omega$ and $v\omega$) are computed from $\hat{u}$, $\hat{v}$ and $\hat{\omega}$ by transforming to real space, forming the products and then transforming back to Fourier space, (pseudo-spectral method). It is not hard to see that the computation of $\hat{\omega}_t$ can be done with five two-dimensional fast Fourier transforms (FFT's). In fact, only four FFT's are needed since one can write (reference Basdevant [2])

$$\psi_x\omega_y - \psi_y\omega_x = ((\psi_x)^2 - (\psi_y)^2)_{xy} - [(\psi_x\psi_y)_{xx} - (\psi_x\psi_y)_{yy}].$$

However, in the calculations presented here the less efficient method was used.

The equations (3.2) can be written in the form of a large system of ordinary differential equations:

$$\frac{d\mathbf{y}}{dt} = \mathbf{F}(\mathbf{y}, t) \tag{3.3}$$

where $\mathbf{y}$ is the vector with components $\hat{\omega}(k_1, k_2)$.

Time stepping is performed using a predictor-corrector applied directly to equation (3.3). Let $\mathbf{y}_n$ denote the approximation to $\mathbf{y}(n\Delta t)$ and $\mathbf{F}_n = \mathbf{F}(\mathbf{y}_n, n\Delta t)$. We use the fourth order Adams predictor-corrector scheme given by

$$\mathbf{y}_p = \mathbf{y}_n + \frac{\Delta t}{12}(23\mathbf{F}_n - 16\mathbf{F}_{n-1} + 5\mathbf{F}_{n-2}) \tag{3.4a}$$

$$\mathbf{y}_{n+1} = \mathbf{y}_n + \frac{\Delta t}{24}(9\mathbf{F}_p + 19\mathbf{F}_n - 5\mathbf{F}_{n-1} + \mathbf{F}_{n-2}). \tag{3.4b}$$

Here $\mathbf{y}_p$ is the result of the Adams-Bashforth predictor, $\mathbf{F}_p = \mathbf{F}(\mathbf{y}_p, (n+1)\Delta t)$ and $\mathbf{y}_{n+1}$ is the corrected value obtained from approximating the implicit Adams-Moulton scheme. A single time step thus requires two evaluations of the right hand side $\mathbf{F}$. The classical fourth order Runge-Kutta method is used to obtain starting values for (3.4). These are required initially and whenever the time step is changed.

For stability reasons one may want to integrate the diffusion term, $\nu\Delta\omega$, in an implicit manner. In the Fourier representation this term is very simple and thus can be easily treated in a fully implicit and accurate manner. We write the equations (3.3) in the following way

$$\frac{d\mathbf{y}}{dt} = \mathbf{G}(\mathbf{y}, t) - \Lambda\mathbf{y} \qquad \Lambda = \mathrm{diag}(..., \nu(k_1^2 + k_2^2), ...).$$

where the right hand side $\mathbf{F}$ has been split with Λ the diagonal matrix corresponding to the diffusion term. This last equation can be written in the form

$$\frac{d}{dt}(e^{\Lambda t}\mathbf{y}) = e^{\Lambda t}\mathbf{G}.$$

Now apply the time stepping procedure (3.4) to this equation viewed in terms of the new dependent variable $e^{\Lambda t}\mathbf{y}$. After division by $e^{\Lambda t}$ the predictor-corrector scheme which results is

$$\mathbf{y}_p = e^{-\Lambda\Delta t}\mathbf{y}_n + \frac{\Delta t}{12}(23e^{-\Lambda\Delta t}\mathbf{G}_n - 16e^{-2\Lambda\Delta t}\mathbf{G}_{n-1} + 5e^{-3\Lambda\Delta t}\mathbf{G}_{n-2}) \tag{3.5a}$$

$$\mathbf{y}_{n+1} = e^{-\Lambda\Delta t}\mathbf{y}_n + \frac{\Delta t}{24}(9\mathbf{G}_p + 19e^{-\Lambda\Delta t}\mathbf{G}_n - 5e^{-2\Lambda\Delta t}\mathbf{G}_{n-1} + e^{-3\Lambda\Delta t}\mathbf{G}_{n-2}). \tag{3.5b}$$

The Runge-Kutta scheme is transformed in a similar fashion. The terms $e^{-\nu(k_1^2+k_2^2)\Delta t}$ are stored and need only be recalculated when Δt changes. These resulting schemes are exact in the absence of the convection terms ($\mathbf{G} = 0$).

The variable time step is chosen by stability and accuracy considerations with Δt chosen to satisfy the condition

$$\mathrm{CFL}_{\min} \leq \quad (|u|_\infty + |v|_\infty)\frac{\Delta t}{\tilde{h}} \quad \leq \mathrm{CFL}_{\max} \tag{3.6}$$

where $\tilde{h} = 2/N$, $(N = \max(N_1, N_2))$. The stability region of the explicit predictor-corrector method (3.4) is shown in figure 1 .

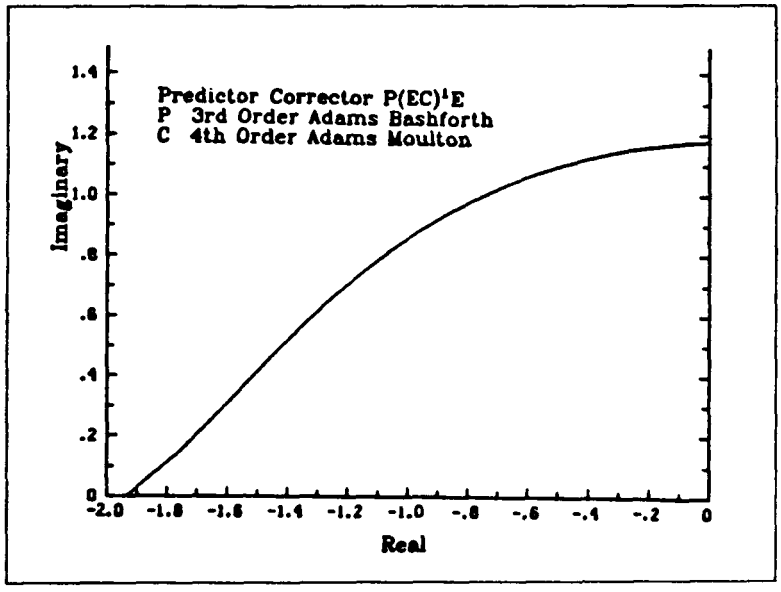

Figure 1 Stability region for the predictor-corrector scheme.

When (3.4) is applied to the model problem $y' = \lambda y$, the time step is restricted by (approximately) $|\lambda|\Delta t \leq 1.2$ if λ is purely imaginary and by $-\lambda\Delta t \leq 1.9$ if λ is real. One expects the implicit predictor-corrector scheme (3.5) to have better stability properties than the explicit one (3.4). $\mathrm{CFL}_{\min}$ and $\mathrm{CFL}_{\max}$ are the minimum and maximum allowable values for the Courant-Friedrichs-Lewy number:

$$\mathrm{CFL} := (|u|_\infty + |v|_\infty)\frac{\Delta t}{\tilde{h}}.$$

$\mathrm{CFL}_{\max}$ would be taken less than the stability limit for the model problem. (The choice of $\tilde{h}$ in our definition of CFL instead of the true $h = 2\pi/N$ means that we can compare CFL directly to the normal stability limit for the model problem.) When the condition (3.6) is violated the new time step is chosen so that

$$(|u|_\infty + |v|_\infty)\frac{\Delta t}{\tilde{h}} = \mathrm{CFL}_{\mathrm{opt}}.$$

3.1 Verification of the Numerical Approximation

In this section we present results which illustrate the accuracy of the numerical approximation that we use. In test 1 we show that the time stepping procedure is accurate to fourth order in Δt. In test 2 we consider the convergence of the numerical solution as the number of modes is increased.

Test 1: Accuracy of the time stepping procedure

It is easy enough to choose the forcing f in the Navier-Stokes equations (3.1) so that the true solution is known to be some given function. Numerous tests of this kind were performed. In all cases the numerical solutions converged to the exact solutions at a rate very close to fourth order in the time step Δt.

As a more realistic study of the convergence of the time stepping routine we consider a sequence of calculations with fixed random initial data and decreasing time steps. The initial conditions are identical with those used in section (3.2) for the decay of random initial data. Keeping the same initial conditions, and with $N_1 = N_2 = 128$, $\nu = 10^{-4}$, the equations were solved with three different (fixed) time steps: $\Delta t = .05$, $\Delta t = .025$ and $\Delta t = .0125$. The computed maximum value for the CFL number in each run was 1.2, .6 and .3, respectively. (Recall that the stability limit for the explicit version of the predictor-corrector scheme is about 1.2 on the imaginary axis. We were able to obtain good results for values of the CFL number as large as 1.5, which substantiates the belief that the implicit predictor-corrector scheme has better stability properties.) We use the results from the three runs to estimate the rate of convergence as a function of Δt as well as to estimate

the actual error. We measure both the discrete maximum error and the l_2 error defined by

$$|\omega|_\infty = \max_{(x_i,y_j)} |\omega(x_i,y_j)| \quad \text{and} \quad |\omega|_2^2 := \frac{1}{N_1 N_2} \sum_{(x_i,y_j)} |\omega(x_i,y_j)|^2.$$

By assuming that the computed solution is converging to the true solution as $O(\Delta t^p)$ we can determine approximate values for p and the errors

$$E_\infty(t,\Delta t) := |\omega_{\text{computed}}(\cdot,t;\Delta t) - \omega_{\text{true}}(\cdot,t;\Delta t)|_\infty = O(\Delta t^p),$$

$$E_2(t,\Delta t) := |\omega_{\text{computed}}(\cdot,t;\Delta t) - \omega_{\text{true}}(\cdot,t;\Delta t)|_2 = O(\Delta t^p).$$

These values are given in table I for the maximum norm errors and in table II for the l_2 errors.

t	$E_\infty(\Delta t = .05)$	$E_\infty(\Delta t = .025)$	$E_\infty(\Delta t = .0125)$	p
10.	0.68×10^{-2}	0.47×10^{-3}	0.32×10^{-4}	3.9
20.	0.27×10^{-2}	0.18×10^{-3}	0.13×10^{-4}	3.9
30.	0.97×10^{-3}	0.69×10^{-4}	0.49×10^{-5}	3.8
40.	0.69×10^{-3}	0.47×10^{-4}	0.32×10^{-5}	3.9
50.	0.48×10^{-3}	0.31×10^{-4}	0.20×10^{-5}	4.0

Table II - Estimated maximum errors and convergence rate: $O(\Delta t^p)$

t	$E_2(\Delta t = .05)$	$E_2(\Delta t = .025)$	$E_2(\Delta t = .0125)$	p
10.	0.40×10^{-3}	0.29×10^{-4}	0.21×10^{-5}	3.8
20.	0.17×10^{-3}	0.12×10^{-4}	0.86×10^{-6}	3.8
30.	0.73×10^{-4}	0.50×10^{-5}	0.34×10^{-6}	3.9
40.	0.56×10^{-4}	0.37×10^{-5}	0.24×10^{-6}	3.9
50.	0.48×10^{-4}	0.31×10^{-5}	0.20×10^{-6}	4.0

Table II - Estimated l_2 errors and convergence rate: $O(\Delta t^p)$

Test 2: Convergence for random initial data

We consider the computation which is described in section (3.2) under the heading of *Run 1: Decay of Random Initial Data.* This computation was run with $N = N_1 = N_2 = 128$ (ω_{128}) and also with $N = 256$ (ω_{256}). The initial conditions for

the two runs were the same to single precision (about $6-7$ decimal digits), although the actual computations were done in double precision. The variable time step was determined by the parameters $(\mathrm{CFL}_{\min}, \mathrm{CFL}_{\mathrm{opt}}, \mathrm{CFL}_{\max}) = (.8, 1., 1.2)$ In table II we indicate the maximum difference and the l_2 difference between the two runs at various times. Due to the variable time step the solutions were not compared at exactly the same times. The difference between the times is given in the table as $t_{256} - t_{128}$. Note that the maximum difference between the two solutions occurs at smaller times. Later on when the solution becomes smoother the errors are smaller. Further details of this run can be found in the next section.

t	$\lvert\omega_{256}\rvert_\infty$	$\lvert\omega_{256} - \omega_{128}\rvert_\infty$	$\lvert\omega_{256} - \omega_{128}\rvert_2$	$t_{256} - t_{128}$
0.	1.00	$.10 \times 10^{-5}$	$.38 \times 10^{-6}$	0.0
10.	.75	$.55 \times 10^{-1}$	$.45 \times 10^{-2}$	$+.42 \times 10^{-5}$
20.	.67	$.20 \times 10^{-1}$	$.29 \times 10^{-2}$	$-.21 \times 10^{-3}$
30.	.60	$.15 \times 10^{-1}$	$.21 \times 10^{-2}$	$+.23 \times 10^{-3}$
40.	.59	$.10 \times 10^{-1}$	$.73 \times 10^{-3}$	$+.18 \times 10^{-4}$
50.	.58	$.73 \times 10^{-2}$	$.58 \times 10^{-3}$	$+.23 \times 10^{-4}$
60.	.57	$.43 \times 10^{-2}$	$.88 \times 10^{-3}$	$-.19 \times 10^{-3}$
70.	.56	$.51 \times 10^{-2}$	$.88 \times 10^{-3}$	$+.25 \times 10^{-3}$
80.	.56	$.26 \times 10^{-2}$	$.38 \times 10^{-3}$	$+.37 \times 10^{-4}$
90.	.56	$.27 \times 10^{-2}$	$.36 \times 10^{-3}$	$+.12 \times 10^{-4}$
100.	.55	$.31 \times 10^{-2}$	$.37 \times 10^{-3}$	$-.62 \times 10^{-4}$

Table II - Convergence of random initial data $\nu = 10^{-4}$

3.2 Computational Results

In this section we present the results of four different runs:

(1) Run I: Decay of random initial data, $\nu = 10^{-4}$, $N = 256$ and $N = 128$.

(2) Run II: Decay of random initial data, $\nu = 10^{-5}$, $N = 512$.

(3) Run III: Decay of smooth random initial data, $\nu = 2 \times 10^{-5}$, $N = 256$.

(4) Run IV: Random forcing, $\nu = .5 \times 10^{-3}$, $\nu = .5 \times 10^{-4}$.

Run I: Decay of random initial data, $\nu = 10^{-4}$, N=256 and N=128.

For the first run we consider the time evolution of the Navier-Stokes equations for *random* initial data. The initial conditions for the vorticity were chosen so that

$$|\hat{\omega}(k_1, k_2)| = \frac{\mathrm{C}}{(k + (\sqrt{\nu}k)^5)}, \quad k = |(k_1, k_2)|,$$

with a random phase. (Actually the initial spectrum was set to zero for all wave numbers above some large value of k.) The constant C was determined by normalizing the maximum value of the vorticity to be 1 at $t = 0$, $|w(\cdot, \cdot, 0)|_\infty = 1$. The value of the viscosity was taken as $\nu = 10^{-4}$ and the number of modes was $N_1 = N_2 = 256$. We show

1) contour plots of the vorticity (figure 2). Dashed lines indicate negative contour values.

2) surface plots of $\hat{\omega}(k_1, k_2)$ in the cosine–sine representation. The discrete Fourier series for $\hat{\omega}$ is actually represented in the computer code as a real series in cosines and sines. The surface plot shows the magnitude of the coefficients of this series. The coefficients are ordered in the following manner:

$$\begin{bmatrix} c_1c_1 & c_1s_1 & c_1c_2 & c_1s_2 & c_1c_3 & \cdots \\ s_1c_1 & s_1s_1 & s_1c_2 & s_1s_2 & s_1c_3 & \cdots \\ c_2c_1 & c_2s_1 & c_2c_2 & c_2s_2 & c_2c_3 & \cdots \\ s_2c_1 & s_2s_1 & s_2c_2 & s_2s_2 & s_2c_3 & \cdots \\ c_3c_1 & c_3s_1 & c_3c_2 & c_3s_2 & c_3c_3 & \cdots \\ \vdots & \vdots & \vdots & \vdots & \vdots & \ddots \end{bmatrix},$$

where c_kc_l is the coefficient of $\cos(kx)\cos(ly)$, c_ks_l the coefficient of $\cos(kx)\sin(ly)$, and so on. The lowest frequency modes are located at the *top* of the surface plot (figure 3). Only the first 128 modes are shown in the surface plots.

3) plots of the energy, enstrophy, J_1, J_2, J_3 as a function of time, and the decay of the vorticity spectrum as a function of k. In figure 4 a we plot the square root of the total energy

$$(1/2(\|u\|^2 + \|v\|^2)^{1/2},$$

the square root of the enstrophy

$$\|w\|,$$

and

$$\nu^{1/2} J_1(t) = \nu^{1/2}(\|\omega_x\|^2 + \|\omega_y\|^2)^{1/2}$$

as functions of time. In figure 4 b we plot the normalized versions of $\nu^{1/2} J_1(t)$, $\nu^{2/2} J_2(t)$ and $\nu^{3/2} J_3(t)$. Recall that

$$J_p^2(t) = \|\frac{\partial^p \xi}{\partial x^p}\|^2 + \|\frac{\partial^p \xi}{\partial y^p}\|^2.$$

In each case the functions plotted are scaled so their maximum value is 1. This maximum value is indicated on the plot as the value of *Scale*. In figure 4 c some selected Fourier coefficients are plotted as functions of time. Finally in figure 4 d we show log–log plots of $\hat{\omega}(k)$ versus k. The quantity $\hat{\omega}(k), k = 1, 2, \ldots$ is defined to be the average value of $|\hat{\omega}(l_1, l_2)|$ over all wave vectors (l_1, l_2) for which k is the closest integer to $l = |(l_1, l_2)|$:

$$\hat{\omega}(k) = \Big(\sum_{|l-k|<1/2} |\hat{\omega}(l_1, l_2)| \Big) / \Big(\sum_{|l-k|<1/2} 1 \Big)$$

We plot $\log_{10}(\hat{\omega}(k))$ versus $\log_{10}(k)$ for different times. Lines with slopes -1 and -2 are also marked. Note that if $\hat{\omega}(k) \sim k^{-\alpha}$ then $E(k) \sim k^{-2\alpha-1}$.

For comparison, in figures 5 - 6 , we show the results of the same run when only half as many modes were used, $N = 128$. Essentially the only noticeable difference is in the plot of the spectral decay. A quantitative comparison of the 256 and 128 runs was given in section (3.1).

Run II: Decay of random initial data, $\nu = 10^{-5}$, $N = 512$.

The value of ν is taken as 10^{-5}. The initial conditions are the same as *Run I*. The number of modes was $N_1 = N_2 = 512$. The results are shown in figures 7 - 8 . Note that for technical reasons the contour plots were made by projecting the solution to a 256×256 grid. It is interesting to compare this run ($\nu = 10^{-5}$) to the previous run ($\nu = 10^{-4}$).

Run III: Decay of smooth random initial data, $\nu = 2 \times 10^{-5}$.

In this run we begin with initial data which is much smoother than in the previous runs. The initial vorticity spectrum is chosen so that

$$|\hat{\omega}(k_1, k_2)| = Ck e^{-\frac{1}{2}(k/k_0)^2} \quad , \quad k_0 = 3.5$$

with random phase. The constant C is chosen so that $|\omega(\cdot, \cdot, 0)|_\infty = 1$. The viscosity was 2×10^{-5} and the number of modes was $N = 256$. These initial conditions are similar to those used by Brachet and Sulem [7]. We have run for longer times than the results shown in [7]. Plots for this run are given in figures 9 - 10 .

Run IV: Random forcing.

In this run we consider the problem when the equations are forced in a range of low Fourier modes. For the forced problem there appears to be no easy way to obtain a sharp bound on the maximum of the vorticity. We have found experimentally that when the forcing is chosen to be $O(1)$ the solution grows and does not remain $O(1)$. For example in figure 11 we show the results of a run in which the forcing f is chosen so that $|f|_\infty = 1$ and in which the initial vorticity is zero. In particular the amplitudes and phases of the the fourier components of the forcing were chosen as

$$\begin{bmatrix} c_1c_1 & c_1s_1 & c_1c_2 & c_1s_2 & c_1c_3 & c_1s_3 \\ s_1c_1 & s_1s_1 & s_1c_2 & s_1s_2 & s_1c_3 & s_1s_3 \\ c_2c_1 & c_2s_1 & c_2c_2 & c_2s_2 & c_2c_3 & c_2s_3 \\ s_2c_1 & s_2s_1 & s_2c_2 & s_2s_2 & s_2c_3 & s_2s_3 \\ c_3c_1 & c_3s_1 & c_3c_2 & c_3s_2 & c_3c_3 & c_3s_3 \\ s_3c_1 & s_3s_1 & s_3c_2 & s_3s_2 & s_3c_3 & s_3s_3 \end{bmatrix} = C_* \begin{bmatrix} +12 & -4 & -16 & +4 & +20 & -12 \\ +8 & -24 & -20 & +12 & +28 & +4 \\ +12 & -8 & +32 & +24 & +8 & +36 \\ -12 & +12 & +4 & +32 & -4 & -16 \\ -4 & -36 & -16 & -36 & -24 & +4 \\ -20 & -20 & -36 & +8 & -28 & +12 \end{bmatrix}.$$

where the scaling factor C_s was chosen to ensure that $|f|_\infty = 1$. In this run $\nu = 10^{-3}$, $N_1 = N_2 = 256$ and $(\mathrm{CFL}_{min}, \mathrm{CFL}_{opt}, \mathrm{CFL}_{max}) = (.5, .8, 1.)$. In figure 11 b we have made plots of the maximum norms

$$\mathrm{MAX(U)} = \max(|u(\cdot,\cdot,t)|_\infty, |v(\cdot,\cdot,t)|_\infty)$$

$$\mathrm{MAX(DU)} = \max(|\frac{\partial u}{\partial x}(\cdot,\cdot,t)|_\infty, |\frac{\partial u}{\partial y}(\cdot,\cdot,t)|_\infty, |\frac{\partial v}{\partial x}(\cdot,\cdot,t)|_\infty, |\frac{\partial v}{\partial y}(\cdot,\cdot,t)|_\infty),$$

and

$$\mathrm{MAX(W)} = |\omega(\cdot,\cdot,t)|_\infty.$$

Even by time $t = 200$ the solution continues to grow.

In contrast when the forcing is chosen to be $O(\nu)$ we do not see growth in the $|\omega(\cdot,\cdot,t)|_\infty$. This observation is presented in figures 12 - 13 where we have made runs with $\nu = .5 \times 10^{-3}$ $(N = 128)$ and $\nu = .5 \times 10^{-4}$ $(N = 256)$. The initial conditions for $|\hat{\omega}|$ were defined by the matrix of coefficients given above but in this case the constant C_s was chosen so that $|\omega(\cdot,\cdot,0)|_\infty = 1$. The forcing was constant in time and defined from the relation

$$\nu\Delta\omega + f = 0.$$

4 Discussion

We have shown that for both two and three dimensional flows the minimum scale, λ_{min}, is essentially proportional to $\nu^{1/2}/|\overline{Du}|_\infty^{1/2}$. We now relate this minimum scale to the decay rate of the energy spectrum.

Let us assume that at a given time t the energy spectrum has a power law behavior in some range of wave numbers, the *inertial range*,

$$E(k) \sim k^{-2\beta}, \qquad k_1 = O(1) \leq k \leq O(1/\lambda_{min}).$$

We have proved that the quantities

$$\frac{\nu^{p-1}}{|Du|_\infty^{p+1}} H_p^2(t) = \frac{\nu^{p-1}}{|Du|_\infty^{p+1}} \left(\|\frac{\partial^p \mathbf{u}}{\partial x^p}(\cdot,t)\|^2 + \|\frac{\partial^p \mathbf{u}}{\partial y^p}(\cdot,t)\|^2 + \|\frac{\partial^p \mathbf{u}}{\partial z^p}(\cdot,t)\|^2 \right)$$

remain of order one, provided they are initially so. When this order one bound is achieved we call the flow *maximal dissipative*. Note that $2\nu H_1^2$ is the rate of energy dissipation, ϵ, and that the rate of enstrophy dissipation η is bounded by νH_2^2.

Assuming that the leading order contribution to the integral for $H_p^2(t)$ is determined from wave numbers in the inertial range and using the power law behavior for $E(k)$ we obtain

$$\frac{\nu^{p-1}}{\overline{|Du|}_\infty^{p+1}} H_p^2(t) \sim \frac{\nu^{p-1}}{\overline{|Du|}_\infty^{p+1}} \int_{k_1}^{1/\lambda_{min}} k^{2p} E(k) dk \sim \frac{\overline{|Du|}_\infty^{-\beta-1/2}}{\nu^{-\beta+3/2}}.$$

In two space dimensions we know that $\overline{|Du|}_\infty$ is essentially bounded by the maximum norm of the initial vorticity. Let us thus assume that the initial values are scaled so that $\overline{|Du|}_\infty$ is of order one. In this case

$$\frac{\nu^{p-1}}{\overline{|Du|}_\infty^{p+1}} H_p^2(t) \sim \nu^{\beta-3/2}, \tag{4.1}$$

and for maximal dissipative flows it follows that $E(k) \sim k^{-3}$, the power law behavior predicted by the Batchelor-Kraichnan theory [3][16].

In three dimensions if we speculate that $\overline{|Du|}_\infty = O(\nu^{-\gamma})$, then

$$\frac{\nu^{p-1}}{\overline{|Du|}_\infty^{p+1}} H_p^2 \sim \nu^{\gamma(\beta+1/2)+\beta-3/2}.$$

In this way for maximal dissipative flows, we obtain a relation between the power law behaviour of the energy spectrum and the size of $\overline{|Du|}_\infty$:

$$\beta = \frac{3-\gamma}{2+2\gamma}.$$

When $\overline{|Du|}_\infty = O(\nu^{-1/2})$, and $\gamma = 1/2$, we obtain $\beta = 5/6$ and $E(k) = k^{-5/3}$, the power law behavior predicted by Kolmogoroff [15].

We now return to the numerical results of the random initial data runs, reference figures 2 - 4 and 7 - 8 . The initial conditions were chosen so that $E(k) \sim k^{-3}$. The numerical results show that this k^{-3} power law seems to remain over an initial time interval. The numerical results further indicate that as the flow evolves, the

quantities $\nu^p J_p^2$, which behave like $\nu^p H_{p+1}$, slowly decrase and the energy spectrum steepens. In a later regime the flow is dominated by the presence of large regions of relatively constant vorticity. There seems to be some evidence from the figures to suggest that the quantities J_p^2 decay by a factor of about $\lambda_{min} = \nu^{1/2}$, and that $\hat{\xi}(k) \sim k^{-1.5}$, $E(k) \sim k^{-4}$. When

$$\frac{\nu^{p-1}}{|D\mathbf{u}|_\infty^{p+1}} H_p^2(t) \sim \nu^{1/2},$$

the argument in (4.1) predicts $\beta = 2$, and is thus consistent with the numerical results. These results are in agreement with Saffman's theory for two dimensional turbulence [22].

In figure 1 we outline an hypothesized behaviour of $\nu^p J_p^2(t)$ for the decay of two-dimensional turbulence. In the first stage of development of the flow, $\nu^p J_p^2$ may show an overall increase as the flow evolves to a state of maximal dissipation. (Of course, depending on the initial data, this maximal dissipative state may never be reached.) This dissipation rate can not continue for a long time interval but must decrease. The power law then slowly changes from k^{-3} to a more rapid decay. The flow becomes organized into coherent structures, a regime with $\nu^p J_p^2 \sim \nu^{1/2}$ (?) and where Saffman's theory would predict $E(k) \sim k^{-4}$. This regime presumably exists for long times, since the viscosity now plays a minimal role. This scenario is suggested by our computations and other similar ones. In particular, Brachet and Sulem [7] show high resolution computation with initial data

$$E(k) \sim ck e^{-(k/k_0)^2},$$

similar to the one presented in this paper (reference figures 9 - 10). They found an increase in the energy power law reaching a maximum at about k^{-3}. At this stage the rate of enstrophy dissipation is maximum, in accordance with our analytical results.

It is conceivable that a similar scenario is present in the decay of three dimensional turbulence. In two dimensions when large coherent structures are formed the main contribution to $H_p^2(t)$ comes from one dimensional layers separating these

structures. When the solutions across the layers have a simple structure, one can argue that that

$$\frac{\nu^{p-1}}{\overline{|D\mathbf{u}|}_\infty^{\,p+1}} H_p^2(t) \sim \lambda_{min} \sim \frac{\nu^{1/2}}{\overline{|D\mathbf{u}|}_\infty^{\,1/2}}.$$

Correspondingly, in three dimensions the same argument can be made assuming that the regions of rapid variation are concentrated along two dimensional structures of width λ_{min}. Thus in either case we obtain a new relation between the power law behaviour of the energy spectrum and the size of $\overline{|D\mathbf{u}|}_\infty = O(\nu^{-\gamma})$:

$$\beta = \frac{2}{1+\gamma}.$$

In two dimensions $\gamma = 0$ and we again obtain $E(k) \sim k^{-4}$. If, in three dimensions $\overline{|D\mathbf{u}|}_\infty \sim \nu^{1/2}$, we obtain $E(k) \sim k^{-8/3}$. Large three dimensional simulations are necessary to confirm the validity of the assumption made on the size of $\overline{|D\mathbf{u}|}_\infty$, on the time evolution of $H_p^2(t)$ and the sharpness of our estimates.

References

[1] J. Barker, *A Numerical Experiment on the Structure of Two-Dimensional Turbulent Flow*, Ph.D. Thesis, Applied Math. Dept., Caltech (1982).

[2] C. Basdevant, *Technical Improvements for Direct Numerical Simulation of Homogeneous Three-Dimensional Turbulence*, J. Comp. Physics 50 (1983), pp. 209-214.

[3] G.K. Batchelor, *Computation of the Energy Spectrum in Homogeneous Two-Dimensional Turbulence*, Phys. Fluid. Suppl. II (1969), pp. 233-239.

[4] R. Benzi, G. Paladini, S. Patarnello, P. Santangelo, A. Vulpiani, *Intermittency and Coherent Structures in Two-Dimensional Turbulence*, J. Phys. A: Math. Gen. 19 (1986), pp. 3771-3784.

[5] M.E. Brachet, D.I. Meiron, S.A. Orszag, B.G. Nickel, R.H. Morf, U. Frisch, *Small-scale Structure of the Taylor-Green Vortex*, J.F.M. 130 (1983), pp. 411-452.

[6] M.E. Brachet, M. Meneguzzi, P.L. Sulem, *Small Scale Dynamics of High Reynolds Number Two Dimensional Turbulence*, subm. to Phys. Rev. Let.

[7] M.E. Brachet, P.L. Sulem, *Direct Numerical Simulation of Two Dimensional Turbulence*, Proc. 4th Beer Sheva of MHD Flows and Turbulence, March 1984, Israel.

[8] B. Fornberg, *A Numerical Study of 2-D Turbulence*, J. Comp. Phys., 25 (1977), pp. 1-31.

[9] D.G. Fox, S.A. Orszag, *Pseudospectral Approximation to Two Dimensional Turbulence*, J. Comp. Phys., 11 (1973), pp. 612-619.

[10] D. Gilbarg, N.S. Trudinger, *Elliptic Partial Differential Equations of Second Order*, Springer Verlag, (1983).

[11] J.R. Herring, J.C. McWilliams, *Comparison of Direct Simulation of Two Dimensional Turbulence with Two-Point Closure: the Effects of Intermittency,* J. Fluid Mech., **153** (1985), pp. 229-242.

[12] J.R. Herring, S.A. Orszag, R.H.Kraichnan, D.G. Fox, *Decay of Two-Dimensional Turbulence,* J. Fluid Mech., **66** (1974), pp. 417-444.

[13] L. Hörmander, *The Boundary Problems of Physical Geodesy,* Arch. Rational Mech. Anal., **62** (1976), pp. 1-52.

[14] M.Y. Hussaini, T.A. Zang, *Spectral Methods in Fluid Dynamics,* Ann. Rev. Fluid Mech., **19** (1987), pp. 339-367.

[15] A.N. Kolmogoroff, C.R.Acad.Sci. U.S.S.R. **30** (1941), pp. 301.

[16] R. Kraichnan, *Inertial Ranges in Two Dimensional Turbulence,* Phys. Fluids, **10** (1967), pp. 1417-1423.

[17] H.O. Kreiss, W.D. Henshaw, L.G. Reyna, *On the Smallest Scale for the Incompressible Navier-Stokes Equations in Two Space Dimensions,* IBM Research Report No.13204 (1987).

[18] H.O. Kreiss, J. Oliger, *Comparison of Accurate Methods for the Integration of Hyperbolic Equations,* Tellus **24** (1972), pp. 199-215.

[19] D.K. Lilly, *Numerical Simulation of Developing and Decaying of Two Dimensional Turbulence,* J. Fluid Mech., **45** (1971), pp. 395-415.

[20] S.A. Orszag, *Analytical Theories of Turbulence,* J. Fluid Mech., **41** (1970), pp. 363-386.

[21] S.A. Orszag, *Numerical Simulation of Incompressible Flows Within Simple Boundaries: I. Galerkin (Spectral) Representation,* Stud. Appl. Math., **50** (1971), pp. 293-327.

[22] P.G. Saffman, *On the Spectrum and Decay of Random Two Dimensional Vorticity Distributions at Large Reynolds Numbers,* Studies Appl. Math., **50** (1971), pp. 377-383.

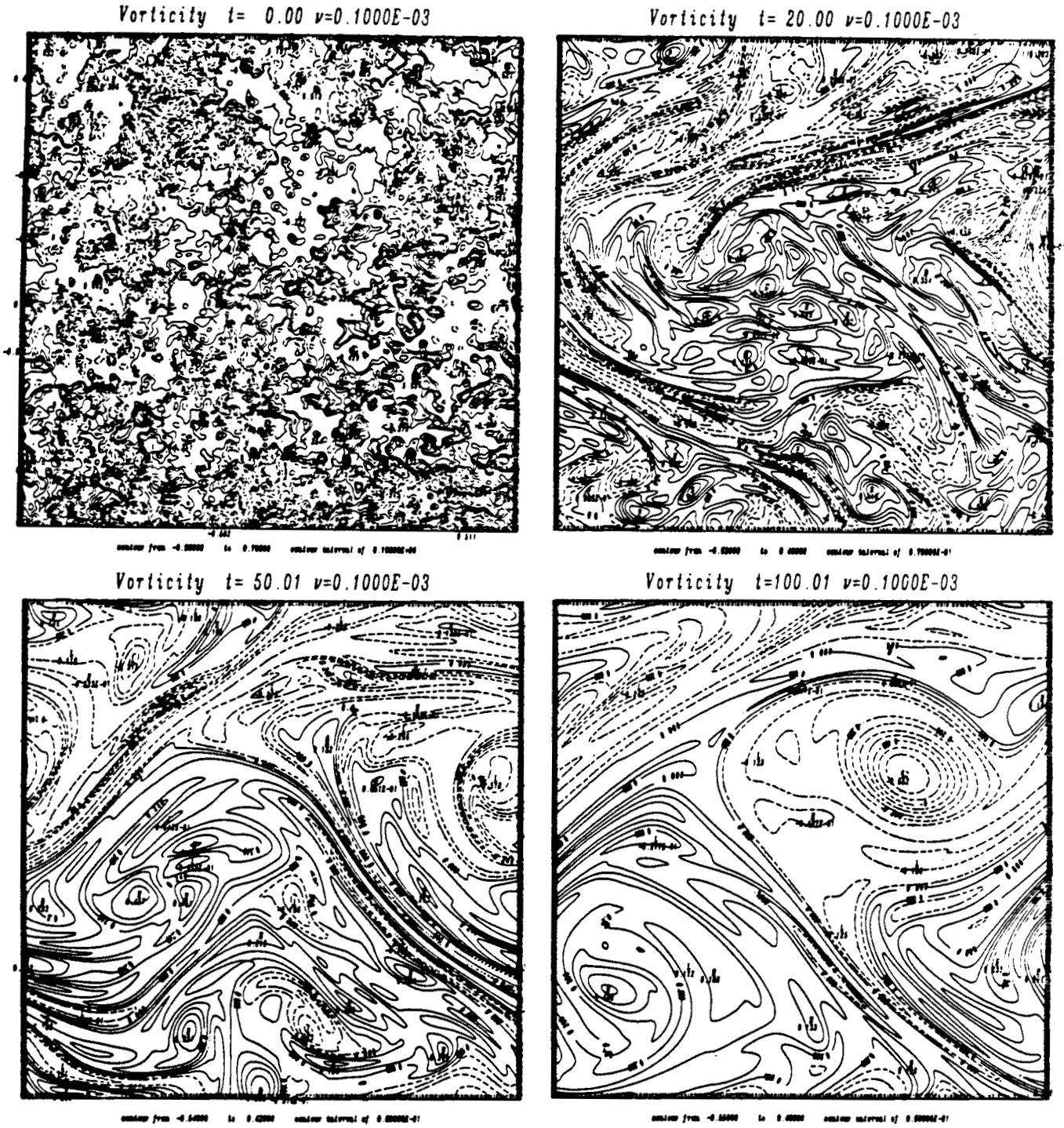

Figure 2 Contour plots of the vorticity for random initial data, $\nu = 10^{-4}$, $N = 256$.

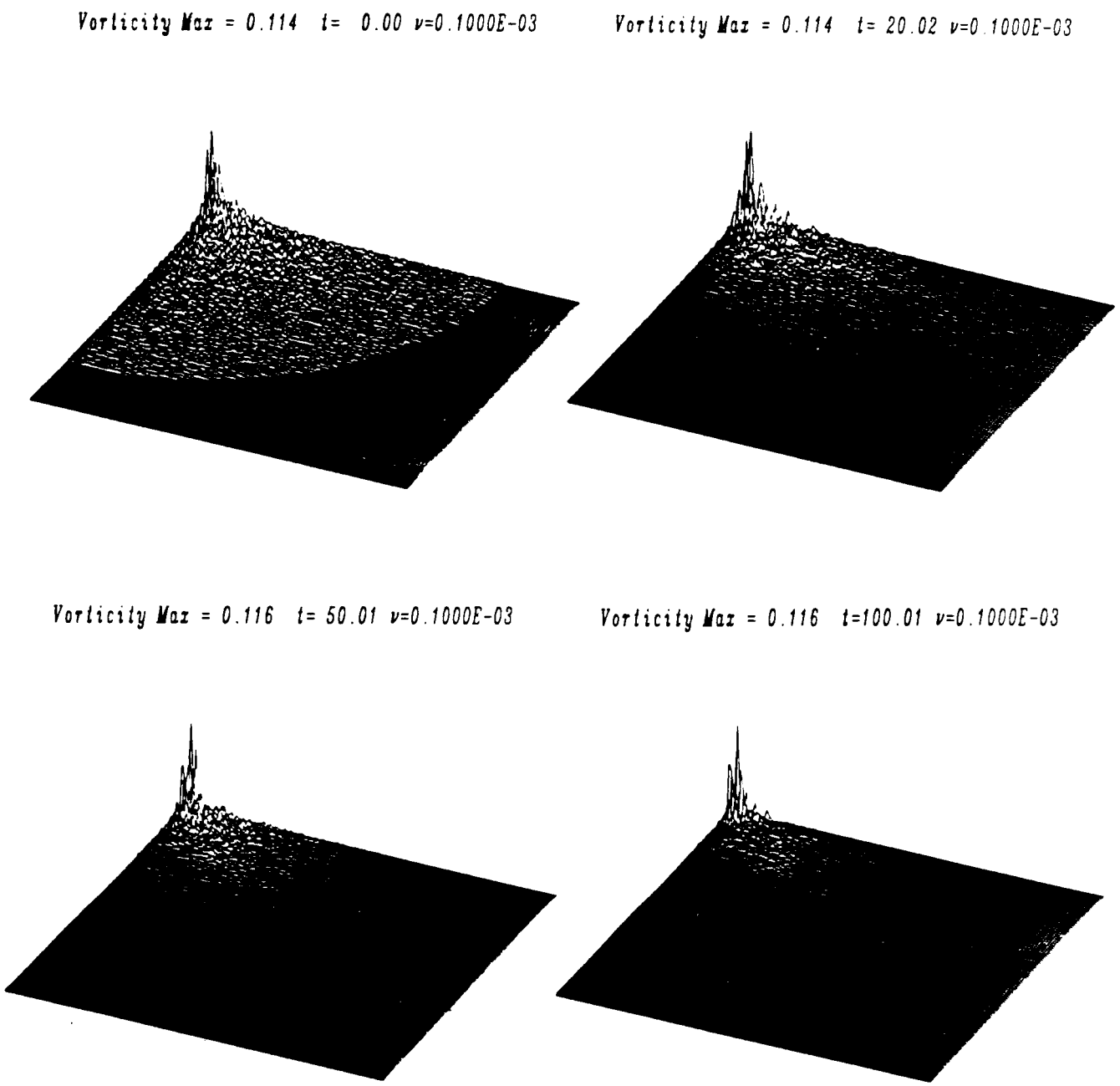

Figure 3 Surface plots of vorticity spectrum for random initial data, $\nu = 10^{-4}$, $N = 256$.

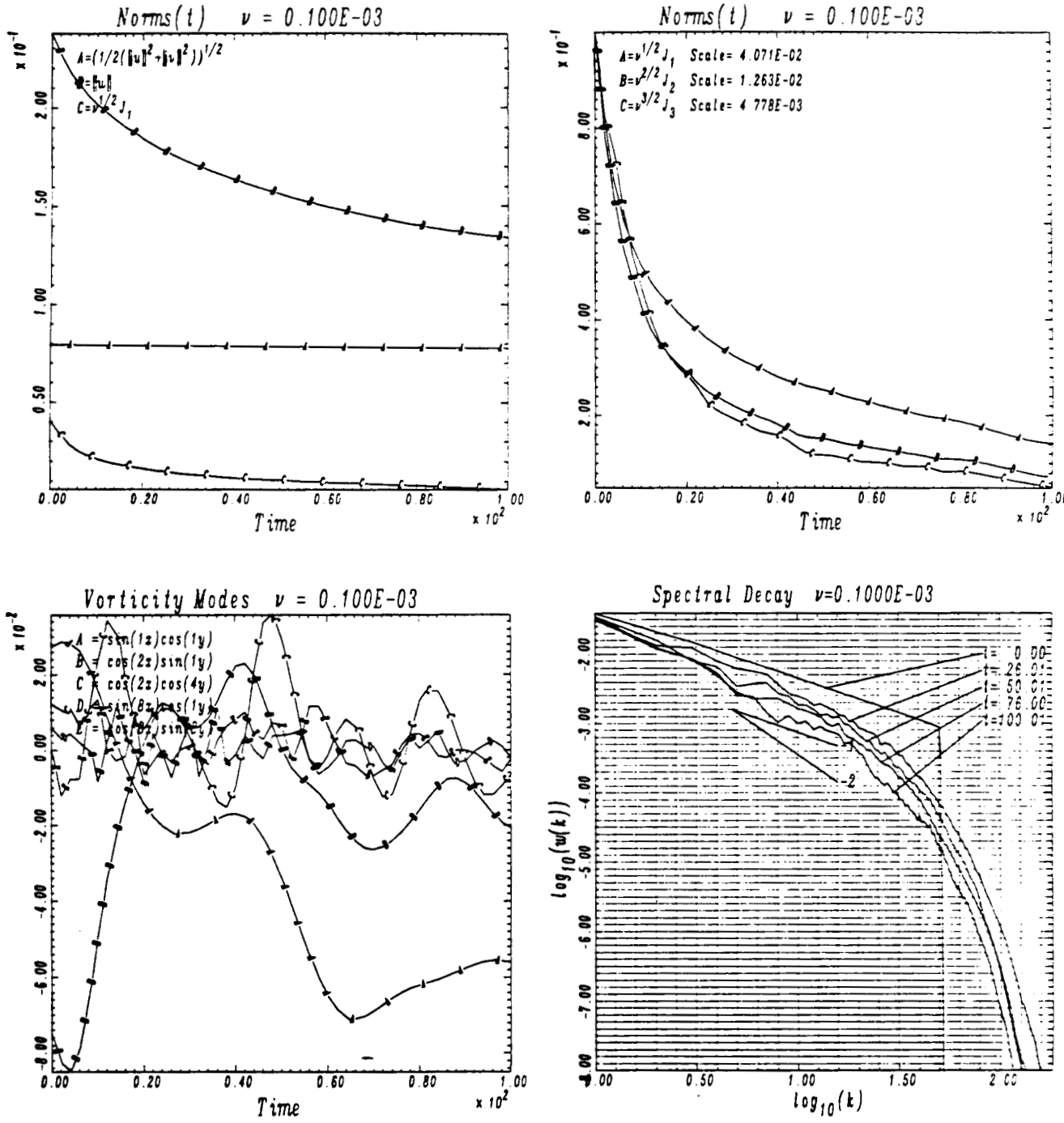

Figure 4 Results for random initial data, $\nu = 10^{-4}$, $N = 256$.

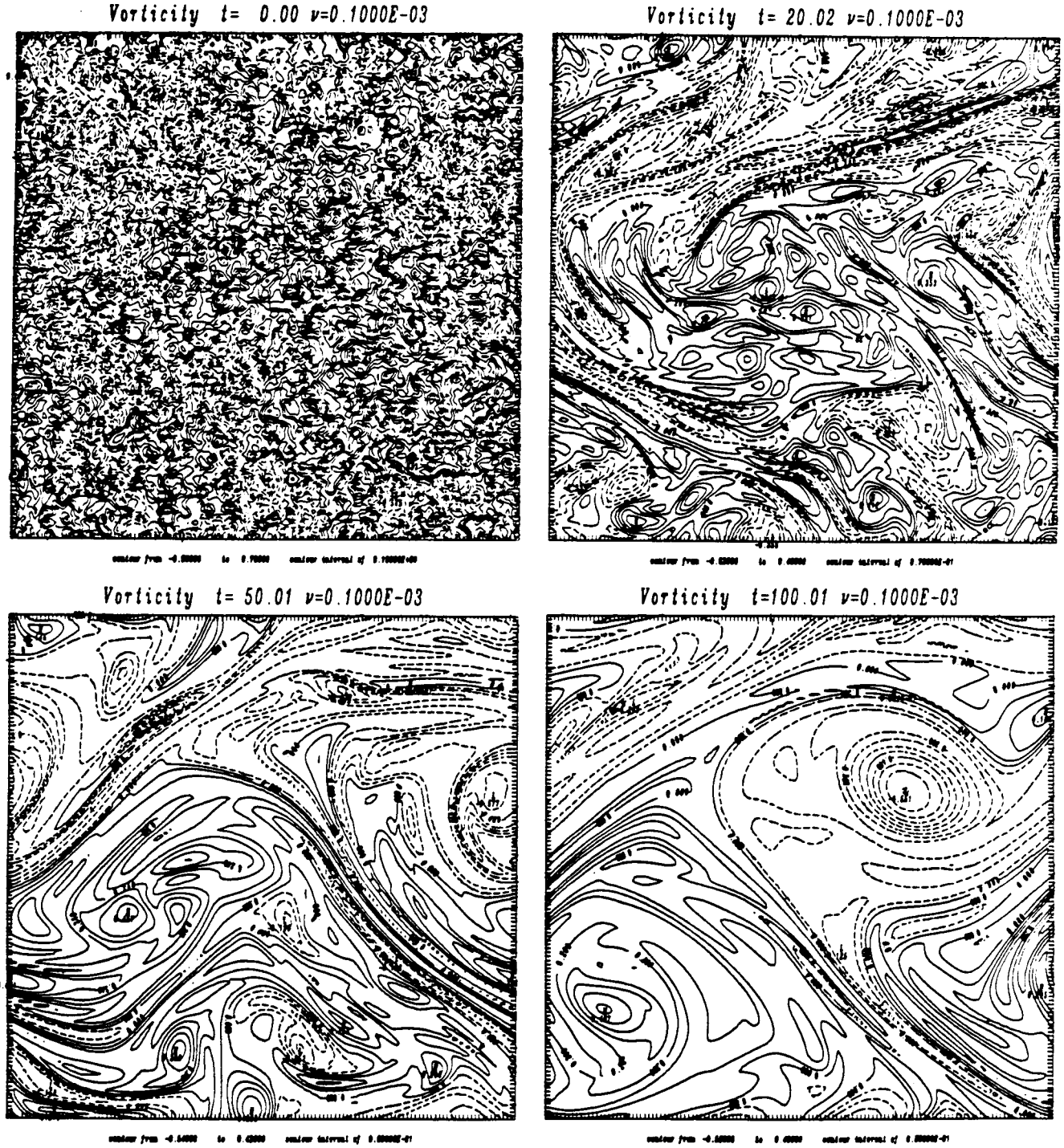

Figure 5 Contour plots of the vorticity for random initial data, $\nu = 10^{-4}$, $N = 128$.

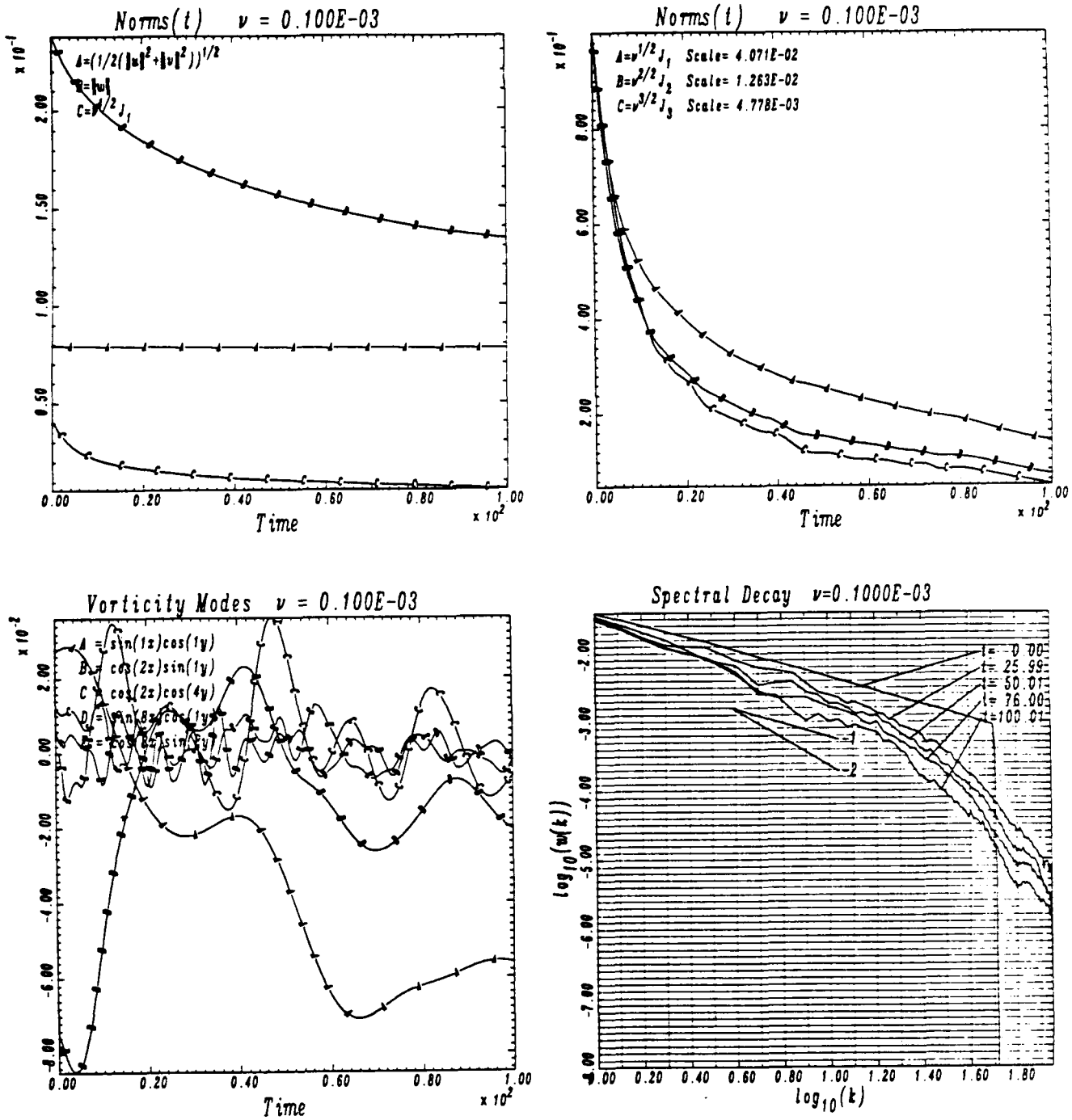

Figure 6 Results for random initial data, $\nu = 10^{-4}$, $N = 128$.

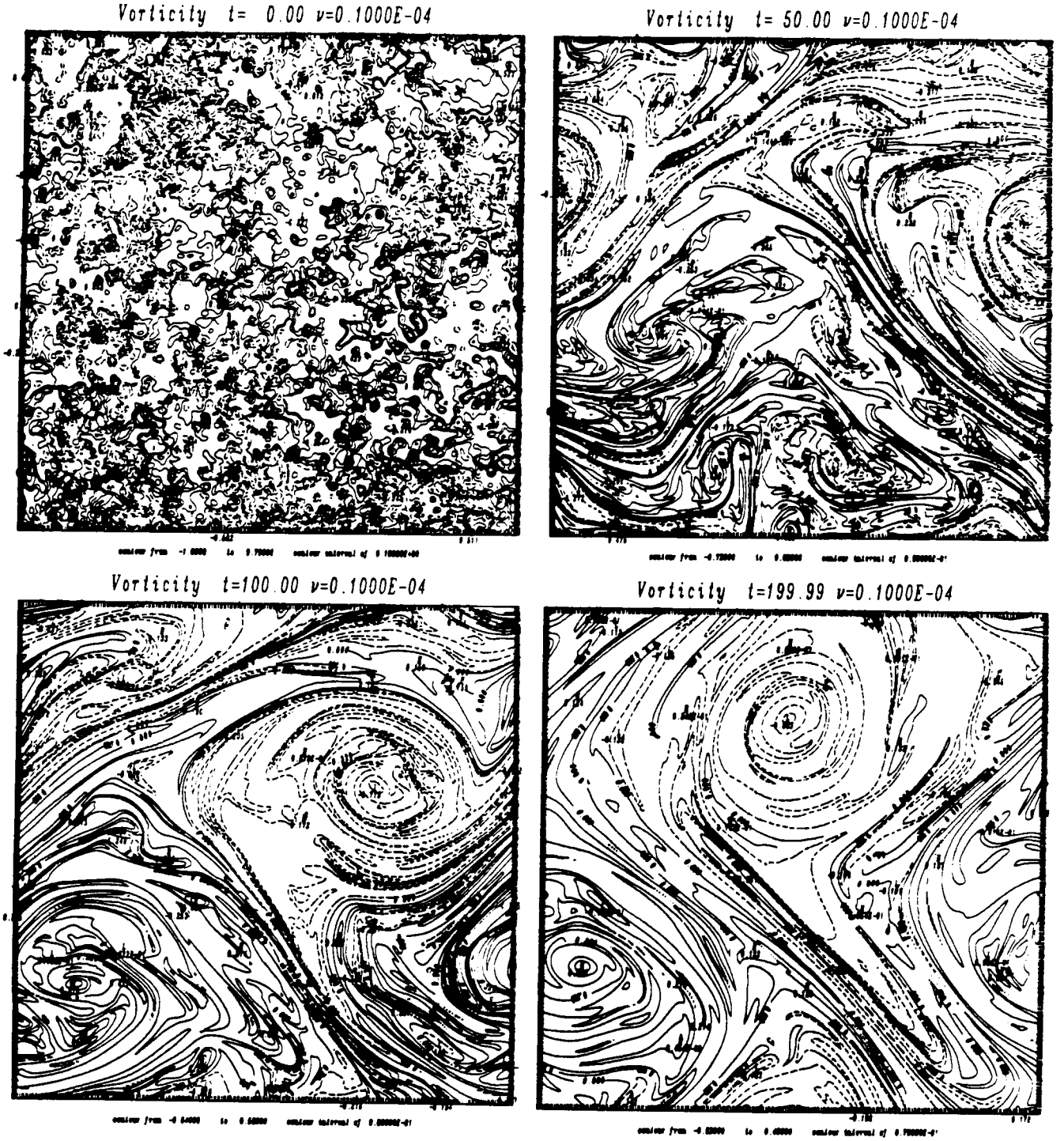

Figure 7 Contour plots of the vorticity for random initial data, $\nu = 10^{-5}$, $N = 512$.

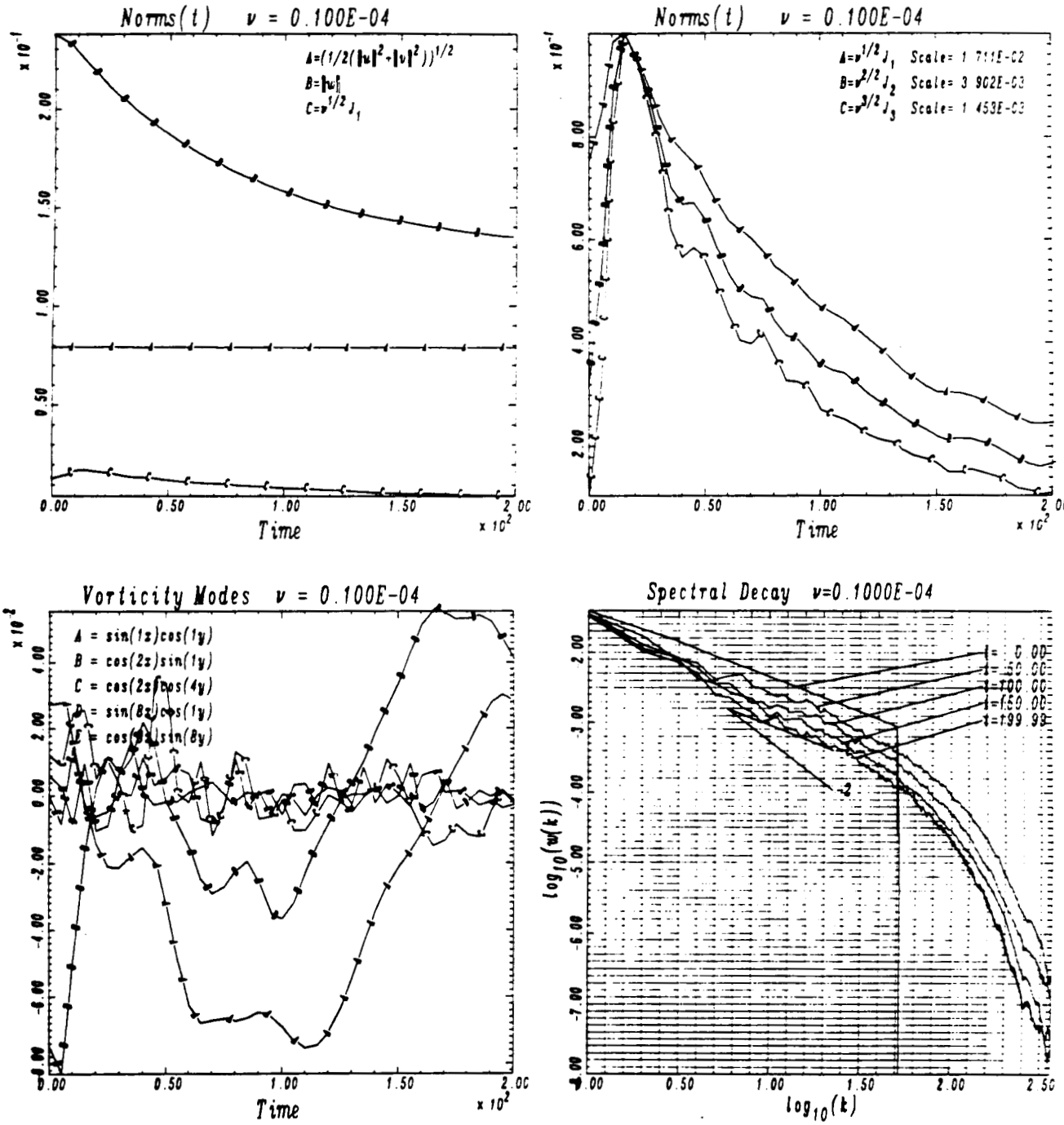

Figure 8 Results for random initial data, $\nu = 10^{-5}$, $N = 512$.

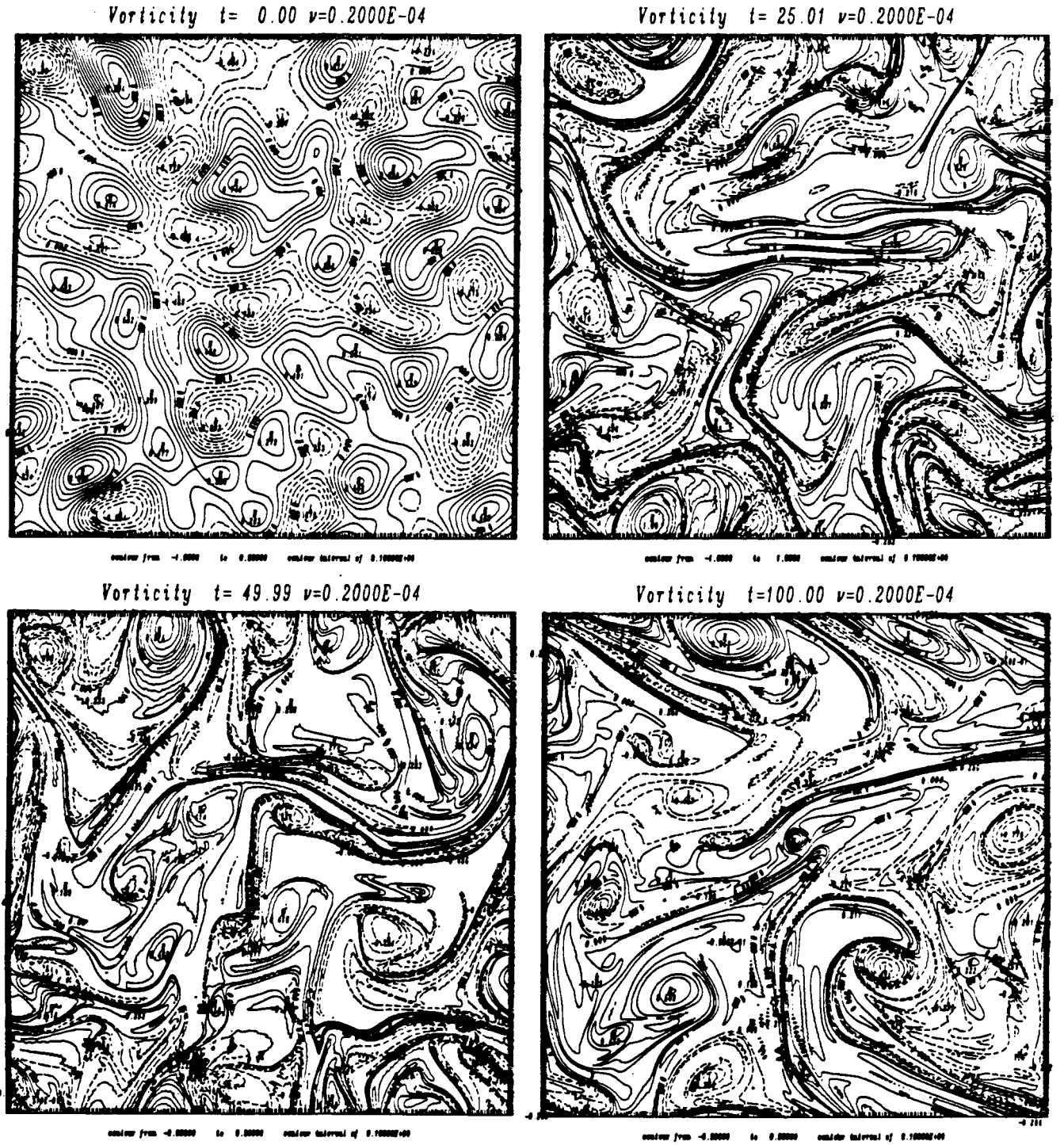

Figure 9 Contour plots of the vorticity for smooth random initial data, $\nu = 2\times10^{-5}$, $N = 256$.

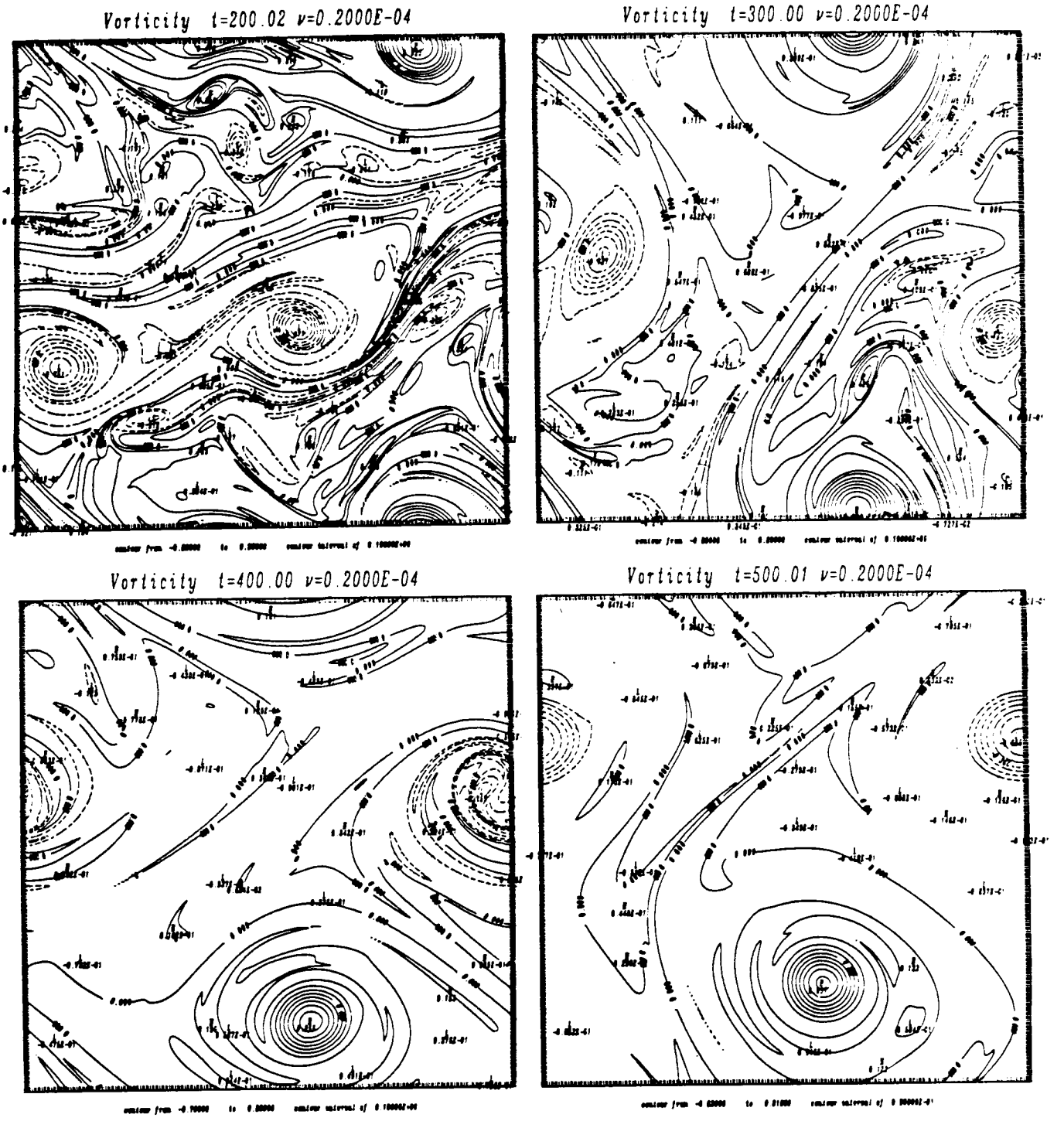

Figure 9 (continued) $\nu = 2 \times 10^{-5}$, $N = 256$.

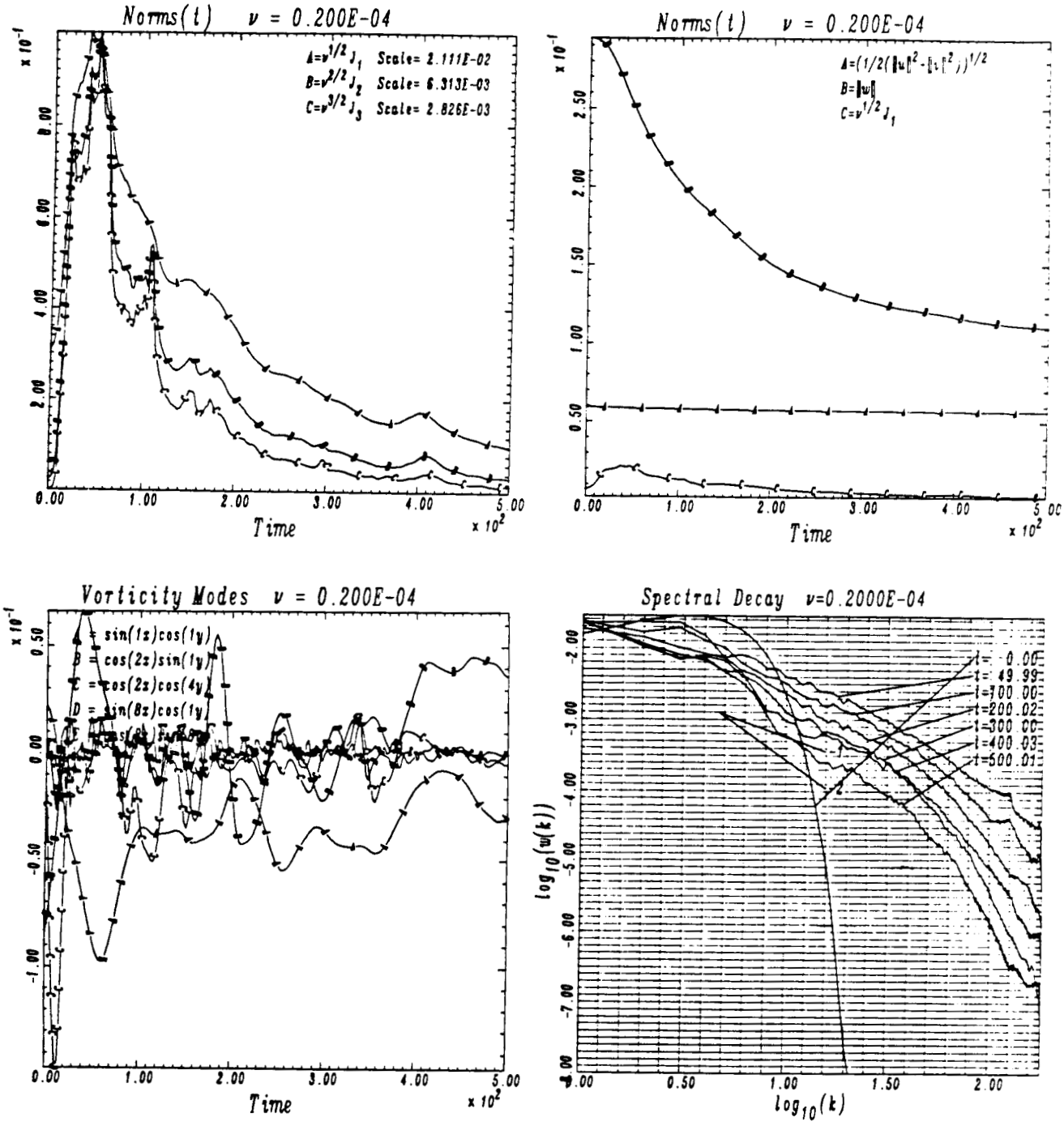

Figure 10 Results for smooth random initial data, $\nu = 2 \times 10^{-5}$, $N = 256$.

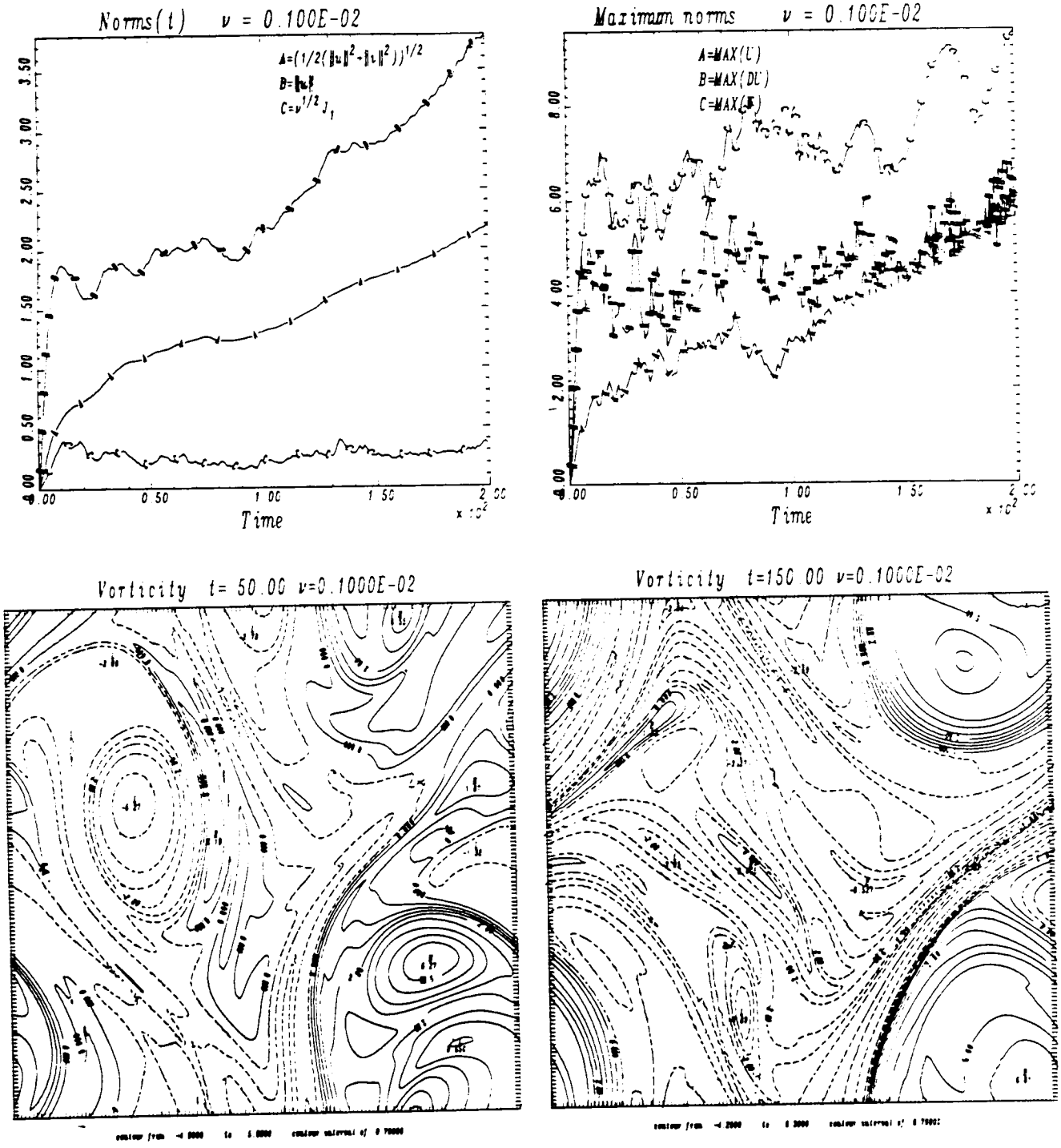

Figure 11 Random Forcing, $|f|_\infty = 1$, $\nu = 10^{-3}$, $N = 128$.

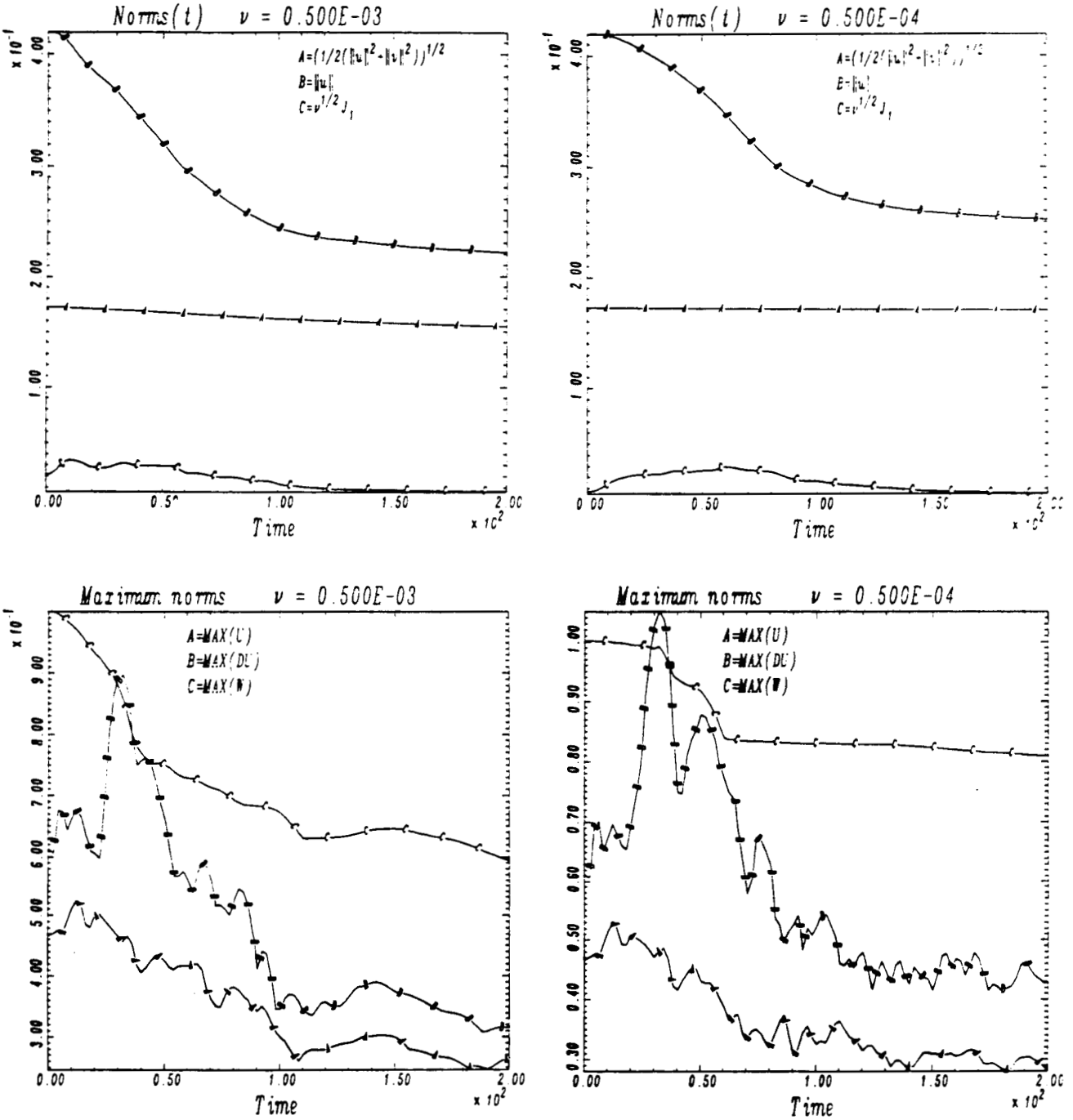

Figure 12 Plots of norms for random forcing, $|f|_\infty = O(\nu)$,
$\nu = .5 \times 10^{-3}$, $N = 128$ and $\nu = .5 \times 10^{-4}$, $N = 256$.

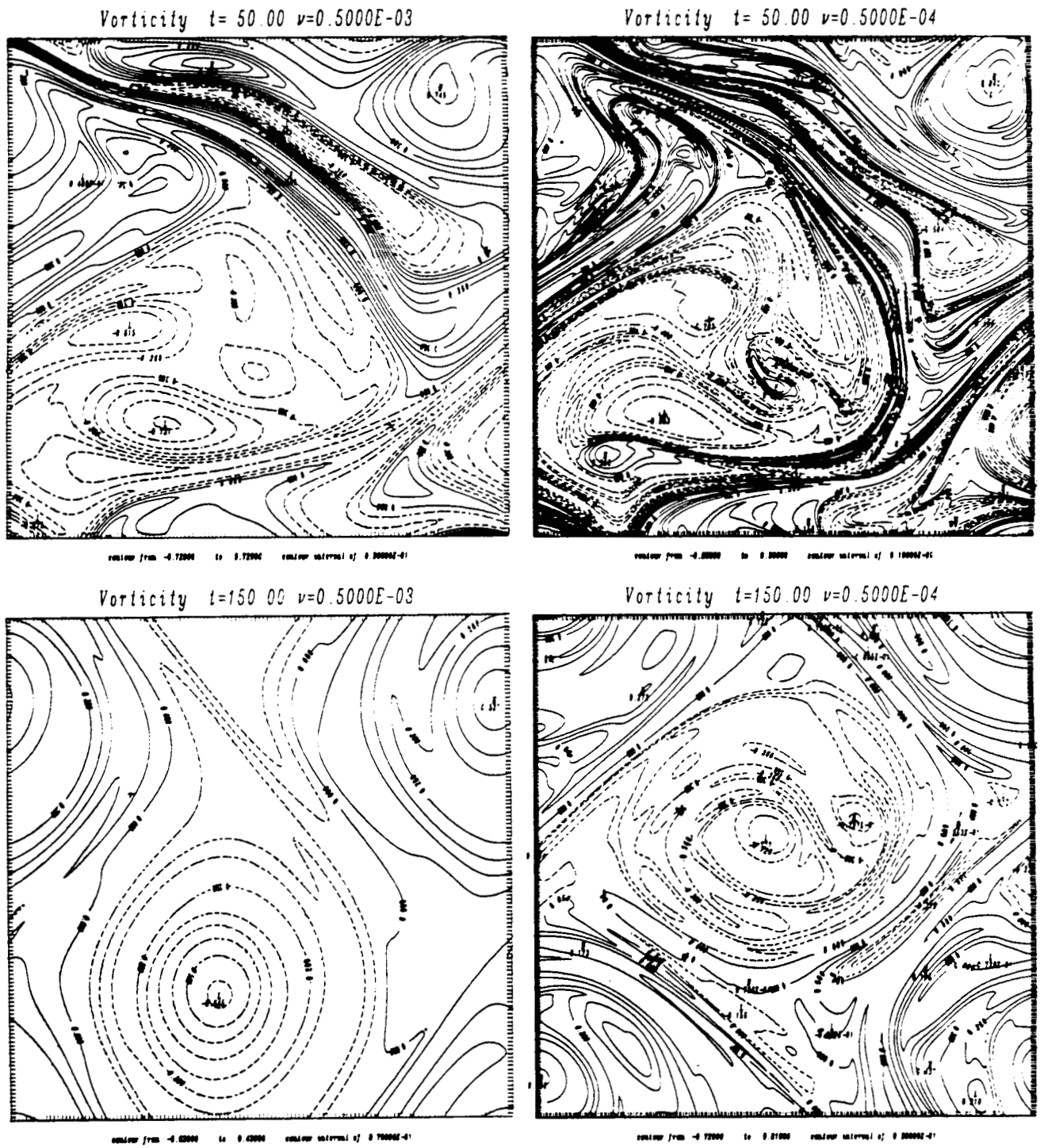

Figure 13 Contour plots of vorticity spectrum for random forcing, $|f|_\infty = O(\nu)$, $\nu = .5 \times 10^{-3}$, $N = 128$ and $\nu = .5 \times 10^{-4}$, $N = 256$.

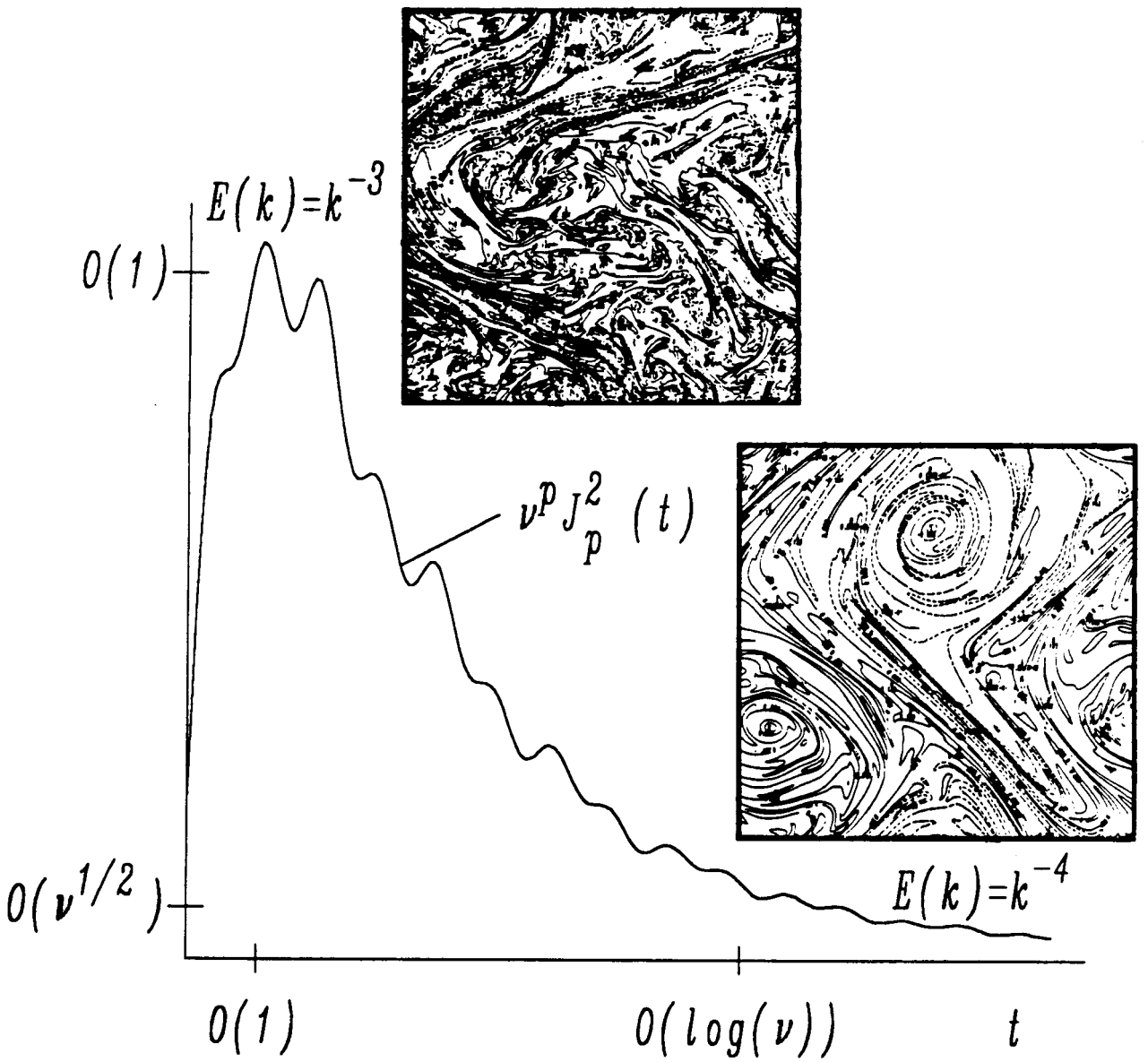

Figure 14 Hypothetical behaviour for $\nu^p J_p^2(t)$

NASA
National Aeronautics and Space Administration

Report Documentation Page

1. Report No.	2. Government Accession No.	3. Recipient's Catalog No.
NASA CR-181628 ICASE Report No. 88-8		

4. Title and Subtitle	5. Report Date
ON THE SMALLEST SCALE FOR THE INCOMPRESSIBLE NAVIER-STOKES EQUATIONS	January 1988
	6. Performing Organization Code

7. Author(s)	8. Performing Organization Report No.
W. D. Henshaw, H. O. Kreiss, L. G. Reyna	88-8
	10. Work Unit No.
	505-90-21-01

9. Performing Organization Name and Address	11. Contract or Grant No.
Institute for Computer Applications in Science and Engineering Mail Stop 132C, NASA Langley Research Center Hampton, VA 23665-5225	NAS1-18107
	13. Type of Report and Period Covered
	Contractor Report

12. Sponsoring Agency Name and Address	14. Sponsoring Agency Code
National Aeronautics and Space Administration Langley Research Center Hampton, VA 23665-5225	

15. Supplementary Notes

Langley Technical Monitor:
Richard W. Barnwell

Submitted to Theoretical and Computational Fluid Dynamics

Final Report

16. Abstract

We prove that for solutions to the two and three dimensional incompressible Navier-Stokes equations the minimum scale is inversely proportional to the square root of the Reynolds number based on the kinematic viscosity and the maximum of the velocity gradients. The bounds on the velocity gradients can be obtained for two dimensional flows, but have to be assumed in three dimensions. Numerical results in two dimensions are given which illustrate and substantiate the features of the proof. Implications of the minimum scale result to the decay rate of the energy spectrum are discussed.

17. Key Words (Suggested by Author(s))	18. Distribution Statement
Navier-Stokes equations, spectral method, turbulence calculation	02 - Aerodynamics 64 - Numerical Analysis Unclassified - unlimited

19. Security Classif. (of this report)	20. Security Classif. (of this page)	21. No. of pages	22. Price
Unclassified	Unclassified	51	A04

NASA FORM 1626 OCT 86